PROBABILISTIC SEISMIC HAZARD ASSESSMENT FOR EARTHQUAKE INDUCED LANDSLIDES

A THESIS SUBMITTED TO
THE GRADUATE SCHOOL OF NATURAL AND APPLIED SCIENCES
OF
MIDDLE EAST TECHNICAL UNIVERSITY

BY

ONUR BALAL

IN PARTIAL FULFILLMENT OF THE REQUIREMENTS
FOR
THE DEGREE OF THE MASTER OF SCIENCE
IN
CIVIL ENGINEERING

JANUARY 2013

Approval of the thesis:

PROBABILISTIC SEISMIC HAZARD ASSESSMENT FOR EARTHQUAKE INDUCED LANDSLIDES

submitted by **ONUR BALAL** in partial fulfillment of the requirements for the degree of **Master of Science in Civil Engineering Department, Middle East Technical University** by,

Prof. Dr. Canan Özgen ________________
Dean, Graduate School of **Natural and Applied Science**

Prof. Dr. Ahmet Cevdet Yalçıner ________________
Head of Department, **Civil Engineering**

Asst. Prof. Dr. Zeynep Gülerce ________________
Supervisor, **Civil Engineering Dept., METU**

Examining Committee Members:

Prof. Dr. Ufuk Ergun ________________
Civil Engineering Dept., METU

Asst. Prof. Dr. Zeynep Gülerce ________________
Civil Engineering Dept., METU

Prof. Dr. Reşat Ulusay ________________
Geological Engineering Dept., Hacettepe University

Prof. Dr. Bahadır Sadık Bakır ________________
Civil Engineering Dept., METU

Asst. Prof. Dr. Nejan Huvaj Sarıhan ________________
Civil Engineering Dept., METU

Date: **25.01.2013**

I hereby declare that all information in this document has been obtained and presented in accordance with academic rules and ethical conduct. I also declare that, as required by these rules and conduct, I have fully cited and referenced all material and results that are not original to this work.

Name, Last name : Onur BALAL

Signature :

ABSTRACT

PROBABILISTIC SEISMIC HAZARD ASSESSMENT FOR EARTHQUAKE INDUCED LANDSLIDES

Balal, Onur
M.S., Department of Civil Engineering
Supervisor: Asst. Prof. Dr. Zeynep Gülerce

January 2013, 61 pages

Earthquake-induced slope instability is one of the major sources of earthquake hazards in near fault regions. Simplified tools, such as Newmark's Sliding Block (NSB) Analysis are widely used to represent the stability of a slope under earthquake shaking. The outcome of this analogy is the slope displacement where larger displacement values indicate higher seismic slope instability risk. Recent studies in the literature propose empirical models between the slope displacement and single or multiple ground motion intensity measures such as peak ground acceleration or Arias intensity. These correlations are based on the analysis of large datasets from global ground motion recording database (PEER NGA-W1 Database). Ground motions from earthquakes occurred in Turkey are poorly represented in NGA-W1 database since corrected and processed data from Turkey was not available until recently. The objective of this study is to evaluate the compatibility of available NSB displacement prediction models for the Probabilistic Seismic Hazard Assessment (PSHA) applications in Turkey using a comprehensive dataset of ground motions recorded during earthquakes occurred in Turkey. Then the application of selected NSB displacement prediction model in a vector-valued PSHA framework is demonstrated with the explanations of seismic source characterization, ground motion prediction models and ground motion intensity measure correlation coefficients. The results of the study is presented in terms of hazard curves and a comparison is made with a case history in Asarsuyu Region where seismically induced landslides (Bakacak Landslides) had taken place during 1999 Düzce Earthquake.

Keywords: Earthquake-induced slope instability, Newmark Sliding Block Analysis, probabilistic seismic hazard assessment, ground motion prediction models, landslide susceptibility

ÖZ

DEPREM KAYNAKLI HEYELANLARIN OLASILIKSAL SİSMİK TEHLİKE ANALİZİ

Balal, Onur
Yüksek Lisans, İnşaat Mühendisliği Bölümü
Tez Yöneticisi: Yrd. Doç. Dr. Zeynep Gülerce

Ocak 2013, 61 sayfa

Deprem kaynaklı şev duraysızlığı problemleri, fay yakınında bulunan bölgelerde deprem tehlikesi yaratan en önemli unsurlardan biridir. Yamaçların deprem etkisi altındaki davranışını modellemek için Newmark Kayan Blok (NKB) analizi gibi basitleştirilmiş yöntemler oldukça yaygın bir biçimde kullanılmaktadır. Bu yöntemin sonucu olan, yamaçtaki yer değiştirme değeri arttıkça, o yamacın deprem altında kayma olasılığı yükselmektedir. Literatürde, yamaç yer değiştirmeleri ile çeşitli kuvvetli yer hareketi değişkenlerini ilişkilendiren görgül modeller bulunmaktadır. Bu modeller, küresel yer hareketi kayıtlarını bir arada bulunduran geniş kapsamlı bir veri bankasından faydalanmıştır. Ancak Türkiye'de gerçekleşen depremlerden elde edilen kuvvetli yer hareketi kayıtları bu veri bankasında yeterli düzeyde temsil edilmemektedir. Bu çalışmanın amacı, Türkiye'de meydana gelen depremler sırasında kaydedilen yer hareketi kayıtlarından oluşan bir veri kümesi kullanarak, mevcut NKB yer değiştirme modellerinin, Türkiye'de uygulanacak Olasılıksal Sismik Tehlike Analizleri (OSTA) için uyumluluğunu değerlendirmektir. Ardından, seçilen uygun NKB yer değiştirme modelinin vektör-değerli OSTA çerçevesinde, sismik kaynak tanımlaması, yer hareketi tahmin modelleri ve yer hareketi parametreleri ölçü ilişkilendirme katsayıları da göz önüne alınarak, uygulaması gösterilmiştir. Bu çalışmanın sonucu olarak, çalışma bölgesi ile ilgili NKB yer değiştirme tehlike eğrileri sunulmuş ve 1999 Düzce Depremi sırasında Asarsuyu Bölgesinde oluşan sismik kaynaklı heyelanlar (Bakacak Heyelanları) ile vaka analizi karşılaştırması yapılmıştır.

Anahtar Kelimeler: Deprem kaynaklı şev duraysızlığı, Newmark kayan blok analizi, olasılıksal sismik tehlike analizi, kuvvetli yer hareketi tahmin denklemleri, heyelan duyarlılığı

to my beloved family…

ACKNOWLEDGEMENTS

I would like to thank my advisor Asst. Prof. Dr. Zeynep Gülerce for her guidance, advice, criticism, and support throughout the preparation of this thesis. I would also like to thank Dr. Norman Abrahamson, for his invaluable guidance in providing the vector-valued hazard code.

I thank to our geologist partner Prof. Dr. Reşat Ulusay for choosing the appropriate region in this study.

I am very grateful to my friends, Recai Soner Ocak, Okan Çağrı Bozkurt, Emre Akyüz and Yiğit Özçelik for their priceless help and support at even the most desperate times during the preparation of this thesis.

I respectfully commemorate my grandfather Hüseyin Çaycı who we have lost during the preparation period of this thesis.

Finally, I am forever indebted to my beloved family Bekir Balal and Birsen Balal who grow me up until now and also Kübra Balal and Osman Anıl Balal who do not avoid their help and support and all of whom give me guidance, understanding and encouragement at any time during my life.

TABLE OF CONTENTS

LIST OF TABLES

TABLES

LIST OF FIGURES

FIGURES

LIST OF ABBREVIATONS

a_y/k_y = Yield Acceleration

a_{max} = Maximum Acceleration

A_{RMS}= Acceleration Root Mean Square

D_n = Newmark Displacement

Dur_{ky} = Duration for which the acceleration is greater than the yield acceleration

ECT = Earthquake Code of Turkey

FS = Factor of Safety

GIS = Geographic Information System

GMPE = Ground Motion Prediction Equation

I_a = Arias Intensity

IM = Intensity Measure

M_w = Moment Magnitude

MRD = Mean Annual Rate Density

MRE = Mineral Research and Exploration

NAFZ = North Anatolian Fault Zone

NEHRP = National Earthquake Hazards Reduction Program

NGA = Next Generation Attenuation

NSB = Newmark Sliding Block

PEER = The Pacific Earthquake Engineering Research Center

PGA = Peak Ground Acceleration

PGV = Peak Ground Velocity

PSHA = Probabilistic Seismic Hazard Analysis (or Assessment)

$Sa_{T=1s}$ = Spectral Acceleration at time equals to 1 second

TSMD = Turkish Strong Motion Database

CHAPTER 1

INTRODUCTION

Earthquake-induced slope instability is one of the major sources of earthquake hazards in near fault regions. In natural and engineered slopes or earth structures, earthquake motions can generate significant horizontal and vertical dynamic forces and increase the shear stresses within the soil mass which may result in the exceedance of shear strength on potential failure planes. Consequently, depending on the characteristics of the slope and strong ground motion, substantial landslide damage may be observed. The damage potential of earthquake-induced landslides is well acknowledged, however, risk-based assessment procedures for this substantial hazard in scenario events, rapid response, and loss estimation is not common practice yet.

Over the past two decades, many scientists had attempted to assess the landslide hazards and produced susceptibility maps portraying their spatial distribution. According to Süzen and Doyuran (2004), basic conceptual model for landslide hazard mapping includes:

- Mapping a set of geological-geomorphological factors that are directly or indirectly correlated with the slope instability,
- Estimating the relative contribution of these factors in generating a slope failure, and
- Classification of land surface into zones of different susceptibility degrees.

Only earthquake-related parameter in this framework is the distance to the fault plane therefore, traditional landslide susceptibility mapping approach misses the important features of scenario earthquakes such as magnitude recurrence relations, ground motion variability, fault activity, seismic moment accumulation, etc. In order to integrate the earthquake-induced landslides in regional event-specific hazard and loss estimates, a complete probabilistic seismic hazard assessment framework should be utilized.

Simplified tools like Newmark's Sliding Block (NSB) Analysis are widely used to represent the stability of slopes under ground shaking. The outcome of this analogy is a quantitative measure, the NSB displacement, where larger displacement values indicate higher seismic slope instability risk. NSB displacement is a suitable parameter for risk based approaches however; NSB Analogy requires extensive computational efforts in large-scaled regional applications. The NSB displacement predictive models avoid the obstacle of selecting suitable input time histories and extensive calculations by estimating the NSB displacement using several ground motion intensity measures and links the earthquake scenarios in the PSHA framework to the earthquake induced landslide hazard.

Using NSB displacement predictive equations, a solid basis could be built for incorporating the earthquake-induced landslide hazards into GIS-based landslide susceptibility assessment studies in regional scales for near-fault regions.

1.1 Research Statement

The main objective of the work done here is to evaluate the compatibility of available Newmark sliding block displacement prediction models for the PSHA applications in Turkey using a comprehensive dataset of ground motions, recorded during earthquakes occurred in Turkey. Six candidate models are selected after initial screening; models proposed by Jibson (2007), Watson-Lamprey and Abrahamson (2006), Bray and Travasarou (2007), Saygılı and Rathje (2008), Bozbey and Gündoğdu (2011) and Hsieh and Lee (2011). The current availability of a much larger set of strong-motion records dictates that the regression models should be updated, so the recent NSB prediction model proposed by Jibson (2007) is selected as the representative model for all the other models proposed by Jibson and his co-workers (Jibson (1993), Jibson et al. (1998), and Jibson (2007)). Recently, Watson-Lamprey and Abrahamson (2006), Bray and Travasarou (2007), and Saygılı and Rathje (2008) proposed NSB displacement prediction models based on The Pacific Earthquake Engineering Research (PEER) Center NGA-W1 database containing a large number of records, therefore, those models are considered as candidate models for Turkey.

Being the only NSB displacement prediction model derived using strong motion records of Turkey, Bozbey and Gündoğdu (2011) model is a natural choice. Hsieh and Lee (2011) model is considered since its dataset includes a large number of strong motions from the 1999 Kocaeli and Düzce earthquakes.

The comparison dataset of Turkey derived by Gülerce et al. (2013) includes 1142 recordings from 288 events with the earthquake metadata, distance metrics for the recordings, and V_{S30} values for the recording stations. However, total number of recordings giving non-zero NSB displacements in the Gülerce et al. (2013) dataset is only 243 for the smallest chosen yield acceleration value (0.02g). Therefore, regionalization of the available global NSB prediction models is preferred instead of developing a new NSB displacement predictive model. Analysis of model residuals method is used to confront the differences between the actual data and the model predictions. A model is considered to be applicable for the probabilistic NSB displacement hazard analysis studies to be conducted in Turkey if: (i) there is no trend observed in the total residual plots for any ground motion parameter or (ii) there is only a constant shift in the total residuals along the zero line which can be easily fixed by changing the constant term of the equation. The most compatible model with the regional ground motion characteristics is found as the Saygılı and Rathje (2008) three parameter vector model.

In the second phase of the study, the application of selected NSB displacement prediction model in a vector-valued PSHA framework is demonstrated. The vector hazard concept for NSB displacement prediction is described in terms of the hazard integral and its main components, since the work performed here is the first study that uses the vector-valued PSHA in Turkey. Correlation coefficients required to implement the vector-valued PSHA including several ground motion intensity measures are presented. Bolu-Düzce Region is selected for the application of the NSB displacement hazard assessment methodology since damaging earthquake-induced landslides were reported in this area during the 1999 earthquakes. The main components of the PSHA framework are the characterization of the seismic sources and the ground motion attenuation relationships. Proper modeling of the seismic sources and suitable ground motion models are employed with the help of available studies for the region (Gülerce and Ocak, 2013 and Levendoğlu, 2013). The results of the analyses are presented in terms of hazard curves, for several locations in the near fault and far-field areas for different site conditions and yield accelerations to assess the effect of these parameters on the final hazard output.

Finally, results of the analyses are compared with a case history in Asarsuyu Region where a seismically induced landslide (Bakacak Landslide) had taken place during 1999 Düzce earthquake. This simple comparison reveals that the method results in the same hazard for all sites at the same distances within the source regardless of the landslide potential, therefore, these analyses should be combined with landslide susceptibility maps. Hazard results would be improved by including the influence of seismic sources falling outside the chosen area. The compatibility of the selected ground motion prediction models with the regional tectonic characteristics should also be evaluated before further analyses. Additionally, the only parameter used in this application that reflects the slope geometry is the yield acceleration, and no other geological-geomorphological factors that can be correlated with the slope instability are considered. Further landslide susceptibility analyses such as evaluating the study area by using aerial photographs for topography, using geological maps and in-situ test for selecting the yield acceleration are required for large-scaled GIS-based probabilistic slope stability risk assessment studies.

1.2 Scope

The scope of the thesis can be summarized as follows;

In the first chapter, after a brief introduction the research statement of the study with the scope is presented.

In Chapter 2, earthquake-induced slope stability assessment methods; pseudostatic approach, Makdisi and Seed Analyses, and Newmark Sliding Block (NSB) analogy are briefly summarized. Global and regional NSB displacement predictive equations are introduced and discussed in terms of datasets and functional forms.

In Chapter 3, predictions of NSB displacement models introduced in Chapter 2 are compared with the actual ground motion intensity measures and NSB displacement values in the comparison dataset of Turkey to find the most compatible model (or models) for the PSHA applications in Turkey.

The vector-valued hazard application for NSB displacement prediction model selected in Chapter 3 is described in terms of the hazard integral and its main components in Chapter 4. NSB displacement hazard curves for several sites in Bolu-Düzce Region are provided for different site conditions and yield accelerations. Estimated NSB displacement hazard curves are compared to a case history, Bakacak Landslide occurred during 1999 Düzce Earthquake.

In the final chapter, a brief summary of the study and discussion of the result is presented. Limitations of the study and future research directions in this field are also discussed in this chapter.

CHAPTER 2

PREDICTIVE MODELS FOR NEWMARK SLIDING BLOCK DISPLACEMENT

Static stability of slopes (excluding the effects of dynamic forces) can be affected by many factors such as geological and hydrological conditions, topography, climate, weathering, and land use. Having a precise slope stability assessment plays an important role in minimizing the damage caused by slope instability and all these factors should be taken into consideration to have an accurate slope stability assessment. Based on the principles and terminology proposed by Varnes (1978), Keefer (1984) categorizes the earthquake induced landslides by material (landslides in rock or soil), character of movement and other attributes such as degree of internal disruption, water content, etc. as given in Table 2.1. Different methods for analyzing each of these instability cases are available in the design manuals, design codes and regulations (i.e. Eurocode 7: Geotechnical Design (1997), Washington State Department of Transportation Geotechnical Design Manual (2012)).

In addition to these important factors, earthquakes can also cause landslides and seismic forces induced by earthquakes call for the dynamic evaluation of slope stability. Two particularly different approaches are available in seismic (or dynamic) evaluation of the slope stability: in *inertia slope stability analysis,* dynamic stresses induced by earthquake shaking are introduced, but in *weakening slope stability analysis,* the effects of dynamic stresses on the strength and stress-strain behavior of slope materials are also taken into account. In other words, inertia slope stability analysis is preferred when material retains its shear strength throughout the ground shaking. However, for the materials that will experience a significant shear strength reduction during an earthquake, weakening slope stability approach is required.

For large-scaled or regional evaluations like this study, the general (inertia) slope stability approach is applicable since the local soil conditions at the analyzed sites are either unknown or roughly estimated and the stress-strain behavior of the soil layers at the sites is not evaluated. In the first part of this chapter, inertia slope stability assessment methods (the pseudostatic approach, Newmark sliding block assessment and Makdisi and Seed (1978) approach will be discussed. Second part of the chapter is focused on the predictive equations for Newmark sliding block displacement, which connects the slope instability analysis to ground shaking parameters. A detailed evaluation of these predictive models, their datasets, functional forms and compatibility with the regional ground motion characteristics will be presented in Chapter 3.

Table 2.1 Movements characteristics of earthquake-induce landslides are summarized by Keefer (1984)

Name	Type of Movement	Internal Disruption*	Water Content**				Velocity	Depth
			D	U	PS	S		
		LANDSLIDES IN ROCK						
		Disrupted Slides and Falls						
Rock falls	Bounding, rolling, free fall	High or very high	X	X	X	X	Extremely rapid	Shallow
Rock slides	Translational sliding on basal shear surface	High	X	X	X	X	Rapid to extremely rapid	Shallow
Rock avalanches	Complex, involving sliding and/or flow, as stream of rock fragments	Very high	X	X	X	X	Extremely rapid	Deep
		Coherent Slides						
Rock slumps	Sliding on basal shear surface with component of headward rotation	Slight or moderate	?	X	X	X	Slow to rapid	Deep
Rock block slides	Translational sliding on basal shear surface	Slight or moderate	?	X	X	X	Slow to rapid	Deep
		LANDSLIDES IN SOIL						
		Disrupted Slides and Falls						
Soil falls	Bounding, rolling, free fall	High or very high	X	X	X	X	Extremely rapid	Shallow
Disrupted soil slides	Translational sliding on basal shear surface or tone of weakened, sensitive clay	High	X	X	X	X	Moderate to rapid	Shallow
Rock avalanches	Translational sliding with subsidiary flow	Very high	X	X	X	X	Very rapid to extremely rapid	Shallow
		Coherent Slides						
Soil slumps	Sliding on basal shear surface with component of headward rotation	Slight or moderate	?	X	X	X	Slow to rapid	Deep
Soil block slides	Translational sliding on basal shear surface	Slight or moderate	?	?	X	X	Slow to very rapid	Deep
Soil earth flows	Translational sliding on basal shear surface with minor internal flow	Slight			X	X	Very slow to moderate, with very rapid surges	Generally shallow, occasionally deep
		Lateral Spreads and Flows						
Soil lateral spreads	Translation on basal zone of liquefied gravel, sand, or silt or weakened, sensitive clay	Generally moderate, occasionally slight, occasionally high			X	X	Very rapid	Variable
Rapid soil flows	Flow	Very high	?	?	?	X	Very rapid to extremely rapid	Shallow
Subaqueous landslides	Complex, generally involving lateral spreading, and/or flow; occasionally involving slumping and/or block sliding	Generally high or very high; occasionally moderate or slight			X	X	Generally rapid to extremely rapid; occasionally slow to moderate	Variable

*Internal Disruption: "slight" signifies landslide consists of one or a few coherent blocks; "moderate" signifies several coherent blocks; "high" signifies numerous small blocks and individual soil grains and rock fragments; "very high" signifies nearly complete disaggregation into individual soil grains or small rock fragments.

**Water Content: D=dry; U=moist but unsaturated; PS=partly saturated; S=saturated.

2.1 EARTHQUAKE INDUCED SLOPE STABILITY ASSESSMENT

Three basic inertial methods for analyzing the earthquake-induced stability of slopes are available in the literature: the pseudostatic approach, Newmark sliding block analysis and Makdisi and Seed (1978) approach.

2.1.1 Pseudostatic Approach

One of the oldest and most commonly used inertial slope stability analyses is the pseudostatic approach. The first explicit application of the method to seismic slope stability has been credited to Terzaghi (1950). The main advantages of this method are the simplicity and ability to consider for both total stress and effective stress parameters. On the other hand, the method ignores the cyclic nature of the earthquakes and handles it as if it is implemented as an additional static force upon the slope. In particular, a lateral force acting through the centroid of the failure mass is applied which acts in out of slope direction as shown in Figure 2.1.

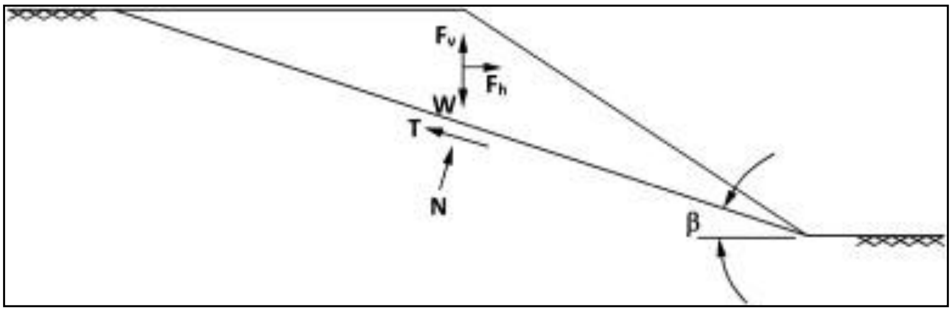

Figure 2.1 Forces acting on a soil wedge in pseudostatic approach

The pseudostatic lateral force (denoted by F_h) is given by:

$$F_h = m \times a = \frac{W \times a_h}{g} = W \times k_h \qquad \mathbf{2.1}$$

where m is the total mass of the slide material (in kg), W is the total weight of the failure mass (in kN), a_h is the horizontal pseudostatic acceleration caused by the earthquake and k_h is the seismic (or pseudostatic) coefficient. It is notable that a slope could be subjected to both vertical and horizontal pseudostatic forces. Since vertical pseudostatic force acting on the sliding mass has a very little effect on its stability, vertical force is usually ignored. Additionally, most earthquakes produce a peak vertical acceleration that is less than the peak horizontal acceleration in both N-S and E-W directions; hence k_v is smaller than k_h (Day, 2002). Equation 2.1 indicates that the earthquake force depends on, the weight of the sliding mass (W) and the seismic coefficient (k_h). Considering the results of field exploration and laboratory testing, unit weight of the sliding mass material can be determined and W can be calculated accurately. The larger the slope failure mass, less likely that during an earthquake the entire slope mass will be subjected to a destabilizing seismic force. Therefore, a lower seismic coefficient should be used as the size of the slope failure mass increases.

Result of the pseudostatic analyses is critically dependent on the precise estimation of k_h. According to Day (2002) and Kumar (2008), k_h can be estimated using the peak ground acceleration (a_{max} or PGA) value or earthquake magnitude but it should never be greater than the value of a_{max} / g. Minimum value of seismic coefficient, suggested by the local design codes may also be used in design (for California k_{hmin}= 0.15 is suggested by Division of Mines and Geology, 1997). Basic rules for estimating k_h proposed by Day (2002) are summarized as follows:

- Terzaghi (1950) suggested k_h= 0.10 for “severe” earthquakes, k_h= 0.20 for “violent and destructive” earthquakes, k_h= 0.50 for “catastrophic” earthquakes.
- Taniguchi and Sasaki (1986) and Krinitzsky et al. (1993) suggested the value of k_h= 0.65 a_{max}/g for slopes of moderate size.
- Marcuson (1981) suggested that for dams k_h ranges between 0.33 a_{max}/g and 0.50 a_{max}/g, but considered possible amplification and deamplification of the seismic shaking due to dam configuration.
- Hynes-Griffin and Franklin (1984) use k_h= 0.50 a_{max}/g for earth dams.

Kramer (1996) stated that the study on earth dams by Hynes-Griffin and Franklin (1984) would be appropriate for most slopes. However, selection of pseudostatic coefficient for slope design should depend on the real expected acceleration level in the failure mass (including any site amplification or deamplification effects). Stewart et al. (2003) reworked the seismic displacement procedure of Bray and Rathje (1998) to advance a rational method to select the seismic coefficient for a pseudostatic screening procedure as a function of the seismic hazard level (i.e., M and rock PGA). In their recent study Bray and Travasarou (2009) proposed that project-specific allowable level of seismic displacement should be established and the site specific seismic demand should be “characterized by the 5% damped elastic design spectral acceleration at the degraded period of the potential sliding mass” either through a deterministic or probabilistic seismic hazard assessment. In this approach, the project performance criteria and the seismic hazard are considered in the choice of the seismic coefficient, k_h.

2.1.2 Newmark Sliding Block Analogy

The pseudostatic approach insures an index of stability (in terms of the factor of safety (FS)) but does not give any information on the deformations associated with the slope failure. As the serviceability of a slope subjected to an earthquake is monitored by post-seismic deformations, a more useful and practical approach of seismic slope stability is provided by slope displacement analyses (Kramer, 1996). Newmark (1965) proposed a simple method to estimate the slope deformations for the case in which the pseudostatic FS is less than unity (i.e. the failure condition). When the FS is less than unity, the potential failure mass is no longer in equilibrium and consequently, it will be accelerated by the unstable force. This aspect is analogous to that of an inclining block (Figure 2.2). This analogy was used by Newmark (1965) to model a potential sliding block of the dam as a rigid plastic single degree of freedom system which can be viewed as a rigid mass resting on an inclined plane. Newmark (1965) assumed that the soil behaves in a-rigid-perfectly-plastic manner in which the movement will only occur when the driving forces due to earthquake base acceleration are sufficient to overcome yield resistance of the block.

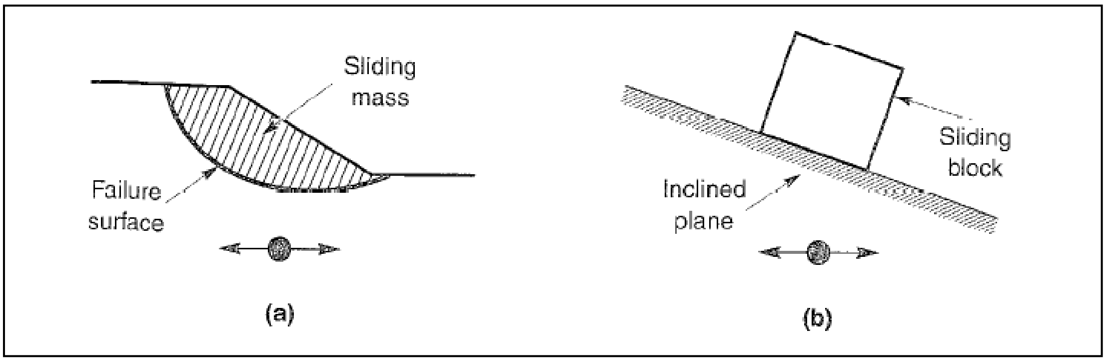

Figure 2.2 Analogy between (a) sliding mass and (b) sliding block on an inclined plane (after Kramer, 1996)

Figure 2.3 (a) shows the acceleration time history which is employed on a slope during an earthquake. A dashed line has been drawn that corresponds to the horizontal yield acceleration that is designated by a_y. This horizontal yield acceleration a_y is considered to be the horizontal earthquake acceleration that results in pseudostatic FS that is exactly equals to 1.0. The two portions of the acceleration pulses that plot above a_y have been darkened, which shows the portions of the time history that will cause lateral slope movements. Figure 2.3 (b) and (c) show the horizontal velocity and displacements calculated by the two darkened portions of an accelerogram. It is notable that the slope displacement is incremental and occurs only when the horizontal acceleration from the earthquake exceeds the yield acceleration. However, a ground motion may exceed the yield acceleration plenty of times and may produce many increments of displacement. In this way, the strong motion duration as well as the frequency content and amplitude will influence the total displacements (Kramer, 1996). The factors that affect the magnitude of the slope displacement can be listed as follows:

- Higher the horizontal yield acceleration a_y, more stable the slope is and thus slope displacement will decrease.
- The peak ground acceleration (PGA= a_{max}) represents the amplitude of the maximum acceleration pulse. More the peak ground acceleration exceeds the yield acceleration, greater the slope displacement.
- Longer the time that earthquake acceleration surpasses the yield acceleration a_y, larger the slope movement.
- More the number of acceleration pulses that exceeds the horizontal yield acceleration a_y, larger the cumulative slope displacement.

Newmark (1965) sliding block analogy involves many assumptions and limitations. One of the major assumptions is: the slope will deform only when ground acceleration exceeds yield acceleration and slope tends to deform as a single massive block which means a rigid-perfectly plastic stress-strain behavior on a planar failure surface. In the field, soils rarely behave as perfectly plastic materials, instead; they usually exhibit strain-hardening or strain-softening behavior after yielding. As a result, the yield acceleration increases due to the changes in the geometry of the unstable soil (Kramer, 1996). However, Keefer (2001) stated that the slope movements, which are basically represented by Newmark (1965) model, can be valid especially for natural slopes, shallow avalanches and soils showing brittle stress-strain behavior (these types of landslides compose more than 90% of total landslides).

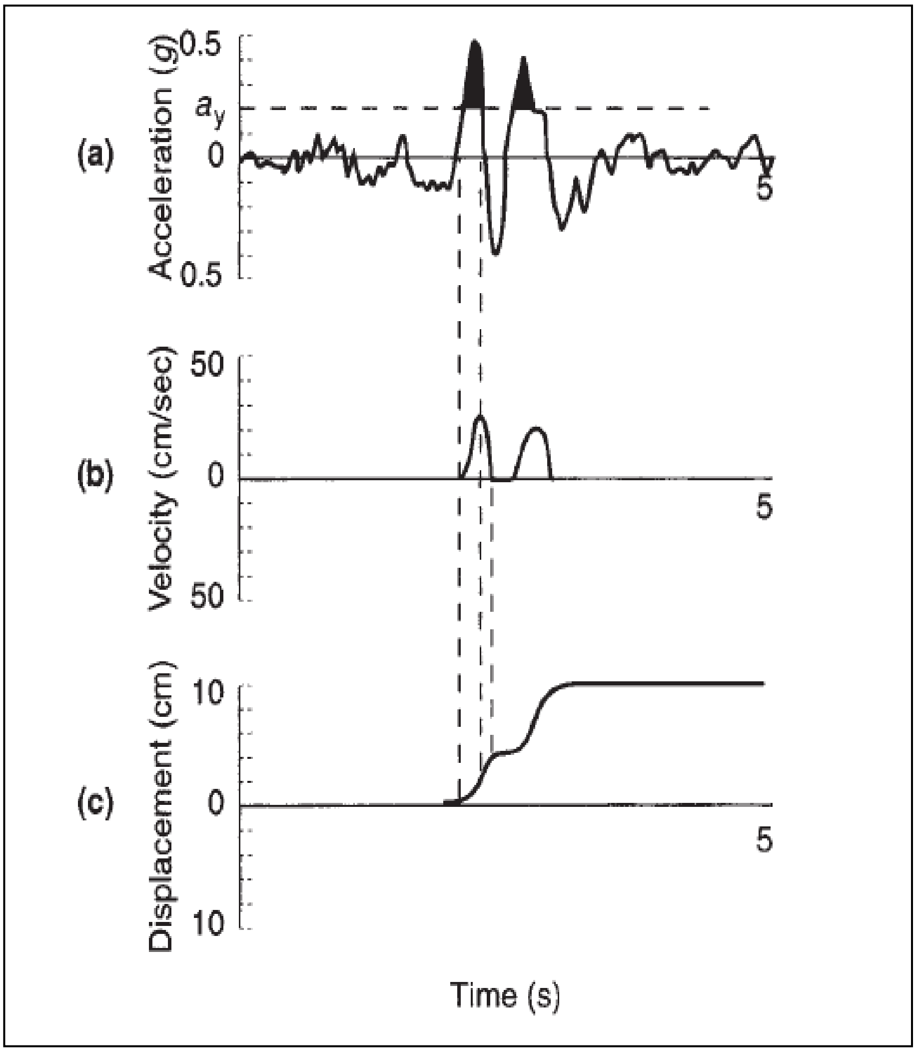

Figure 2.3 Diagram illustrating calculation of the Newmark displacement: (a) acceleration vs. time (b) velocity vs. time for the darkened portions of the acceleration pulse and (c) corresponding downslope displacement vs. time in response to velocity pulses (After Wilson and Keefer, 1985).

2.1.3 Makdisi – Seed Analysis

Makdisi and Seed (1978) used average accelerations calculated by Chopra (1966) and Newmark (1965) to compute the earthquake-induced permanent deformations. From that analysis of the performance of embankments during strong earthquakes, two distinct types of behaviors may be discerned (Kramer, 1996):

a. *The behavior associated with loose to medium dense sandy embankments*: These materials are susceptible to rapid increases in pore pressure due to cyclic loading; resulting in the development of pore pressures equal to the overburden pressure in large portions of the embankment, associated reductions in shear strength, and potentially large movements leading to almost complete failure

b. *The behavior associated with cohesive clays, dry sands, and some dense sands*: Here the potential for build-up of pore pressures is much less than that associated with loose to medium dense sands, the resulting cyclic strains are usually quite small, and the material retains most of its static undrained shearing resistance so that the resulting post-earthquake behavior is a limited permanent deformation of the embankment (Makdisi and Seed, 1978).

By implementing some real and synthetic ground motions, that are scaled to represent different earthquake magnitudes, to the analyses of some real and hypothetical dam structures, Makdisi and Seed (1978) computed the alterability of permanent displacement with a_y/a_{max} and magnitude. By normalizing the displacement with respect to the PGA and the fundamental period of the embankment/dam, scatter in the predicted displacements was reduced and a simplified procedure was developed. In this simplified method:

a. The yield acceleration (a_y) that produces a safety factor equals to 1.0 is determined by pseudostatic slope stability analyses.

b. The maximum crest acceleration, $a_{max,z=0}$ and first natural period, T_o corresponding to a specified earthquake is estimated using computer programs, observations, or literally available approximations.

c. a_{max} is estimated using Figure 2.4 as average for specified sliding mass.

d. The permanent displacement (u) is calculated using Figure 2.5 according to specified magnitude ranges.

It is also worth to mention that material's strength loss potential has to be considered to use Makdisi and Seed (1978) simplified procedure. If significant losses are observed, it is wiser not to use the method however, up to 20% reduction of the static undrained strength can be accepted as a reasonable limit (Bray, 2007).

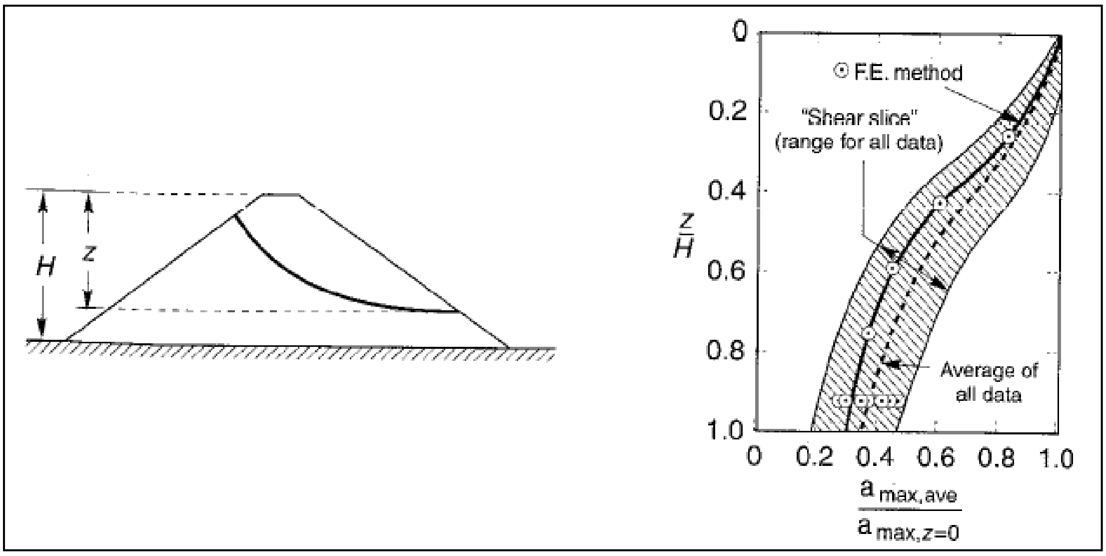

Figure 2.4 Variation of average maximum acceleration with depth of potential failure surface (After Makdisi and Seed, 1978).

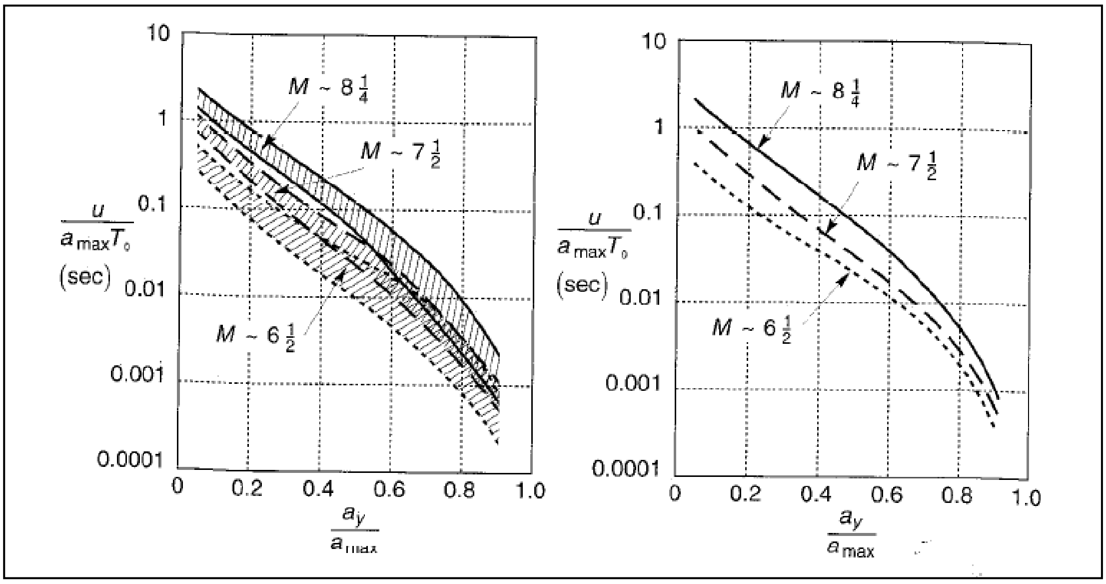

Figure 2.5 Variation of permanent displacement with yield acceleration for different magnitude earthquakes: (1) summary for several earthquakes and dams; (2) average values (After Makdisi and Seed, 1978).

2.2 Newmark Sliding Block Displacement Predictive Models

"Most moderate and large earthquakes trigger landslides and in many cases these landslides account for a significant proportion of total earthquake hazard" (Jibson, 2007). Estimating where earthquake induced landslides are possibly to happen and what sort of conditions will trigger the landslides is a considerable topic in regional seismic hazard assessment. Methods for anticipating slope displacements during earthquakes have been developing substantively since Newmark (1965) first presented a simple model, still used commonly, to predict co-seismic slope displacement.

Newmark (1965) analyzed simple acceleration time histories of four real cases to gather a graphical generalization to estimate displacement as a function of the critical acceleration to the maximum acceleration ratio (a_y/a_{max}). This term is referred as the critical acceleration ratio. Same approach was followed by Sarma (1975), Franklin and Chang (1977), Hynes-Griffin and Franklin (1984), Lin and Whitman (1986), and Yegian et al. (1991) to improve displacement estimates using a variety of simple shaped acceleration time histories (e.g., sinusoidal, or triangular) additionally with the larger collections of real strong motion recordings. All of these simplified models plotted Newmark sliding block (NSB) displacement with respect to critical acceleration ratio, and some recommended simple equations for defining the upper limits of NSB displacements. Wilson and Keefer (1983) applied Newmark's method to a real case that happened by the Coyote Creek, 1979 earthquake. The slide occurred near a strong-motion instrument, and the landslide displacement predicted in the Newmark analysis using the record from that instrument agreed well with the real case. These preliminary results encouraged the researchers to use Newmark displacement as a proxy to determine the seismic landslide hazard and risk in near-fault regions.

2.2.1 Early-Stage Prediction Models

Newmark analysis were first used by Wieczorek et al. (1985) as a basis for landslide microzonation caused by earthquakes and methods for such applications have been developed since that study (e.g., California Division of Mines and Geology, 1997; Jibson et al., 1998; Mankelow and Murphy, 1998; Luzi and Pergalani, 1999; Miles and Ho, 1999; Jibson et al., 2000; Miles and Keefer, 2000, 2001; Del Gaudio et al., 2003; Rathje and Saygılı, 2006) most of which contain GIS implementations. In these implementations, areas of interest are gridded and for each grid cell co-seismic separate displacements are obtained. To carry out a careful Newmark analysis for each grid cell a selection of unique strong-motion history for every cell is necessitated, which is hard to apply. Furthermore, simple empirical predictive equations which estimate NSB displacement as a function of different ground motion parameters ease faster and more accurate GIS-based seismic landslide micro-zonation (Jibson, 2007).

One of the earlier predictive models for the Newmark displacement (D_n) was proposed by Ambraseys and Menu (1988). Their model estimates D_n as a function of the critical acceleration ratio based on the analysis of 50 strong-motion records from 11 earthquakes.

Empirical models in different functional forms have been proposed by Yegian et al. (1991), Jibson (1993), Ambraseys and Srbulov (1994, 1995), and Crespellani et al. (1998) with some other parameters included to predict D_n. These models were developed based on limited datasets and the resulting predictive equations displayed very large variabilities.

Among the others, the most widely used model was the one which is proposed by Jibson (1993) for yield acceleration (a_y) values of 0.02g, 0.05g, 0.10g, 0.20g, 0.30g, and 0.40g based on 11 strong-motion records. This model has a robust goodness of fit value (R^2= 0.87), however it is rather sensitive to small changes in a_y.

Jibson et al. (1998) modified the functional form of the Jibson (1993) model by using logarithmic terms and enlarged the size of the database tremendously (555 strong-motion records compiled from 13 earthquakes) which eventually increased the aleatory variability (R^2= 0.83).

In his recent work, Jibson (2007) handled this increase in variability by adding other parameters in the predictive model as well as compiling a comprehensive dataset (2270 strong-motion records compiled from 30 earthquakes). He concluded that the NSB displacement prediction models should take into account 4 main factors: (1) the critical acceleration ratio, (2) the critical acceleration ratio combined with magnitude, (3) the Arias intensity, I_a (Arias, 1970) combined with critical acceleration, and (4) the I_a combined with critical acceleration ratio. These factors can be represented by four basic parameters: I_a, critical acceleration, PGA or the maximum acceleration of the acceleration time history, and the moment magnitude of the earthquake. As a result, Jibson (2007) derived separate predictive models for all four main factors.

2.2.2 Prediction Models Based on the PEER Database

NSB displacement prediction model proposed by Watson-Lamprey and Abrahamson (2006) was derived using The Pacific Earthquake Engineering Research (PEER) Center NGA-W1 database containing 6158 records from 175 earthquakes and these records were scaled by seven different scale factors (0.5, 1, 2, 4, 8, 16 and 20) resulting in a dataset of 43106 records. Watson-Lamprey and Abrahamson (2006) included four ground motion parameters (Spectral Acceleration with 5% damping at 1 second, Acceleration Root Mean Square, Peak Ground Acceleration, and the duration) in the prediction equation and used random effects regression to build the model.

Bray and Travasarou (2007) had also taken the advantage of the PEER-W1 database, which provides the opportunity to characterize the influence of ground motions on the seismic performance of a slope accurately. The ground motion dataset used by Bray and Travasarou (2007) includes records from shallow crustal earthquakes that occurred in active plate margins satisfying the following criteria: (1) $5.5 \leq M_w \leq 7.6$, (2) $R \leq 100$ km, (3) recorded on simplified geotechnical sites B, C, or D (i.e., rock, soft rock/shallow stiff soil, or deep stiff soil, respectively, Rodriguez-Marek et al., 2001), and (4) frequencies in the range of 0.25 to 10

Hz have not been filtered out (total number of 688 records from 41 earthquakes). To calculate the average seismic displacement two horizontal components of every record were used by flipping the records (polarity effect) and maximum of these values was assigned to that record. As a result, Bray and Travasarou (2007) choose three ground motion parameters (The Initial Fundamental Period of the Sliding Mass (T_s), Spectral Acceleration at a period of 1.5 T_s with 5% damping at 1 second, and moment magnitude) in the prediction equation and used random effects regression to build the model.

Saygılı and Rathje (2008) proposed both scalar and vector valued (using multiple ground motion parameters) predictive equations in an effort to reduce the standard deviation of the NSB displacement prediction model. Their subset of PEER database includes ground motions from earthquakes ranging from moment magnitude between 5 to 7.9 and distances from 0.1 to 100 km. Ground motions recorded at soft soil sites, on the crest or abutments of dams, underground, not at the ground floor of a building, or in buildings larger than 4 stories were removed from the dataset. Additionally, ground motions with high-pass filter corner frequencies larger than 0.25 Hz or low-pass filter corner frequencies less than 10 Hz were removed, resulting in a dataset including 2383 ground motions. Approximately 25% of the initial ground motion data set had PGA values of less than 0.05 g which is the minimum yield acceleration value used in the analyses, therefore these motions do not result in any NSB displacement. To further populate the database at larger values of PGA, NSB displacements were also calculated for each ground motion scaled by factors of 2.0 and 3.0. To ensure that unreasonable PGA values were not created while scaling, the ground motions were capped at PGA= 1.0g. The final NSB displacement data set when capping at PGA= 1.0g included approximately 14,000 nonzero displacements that were used in the regression analysis. The computed displacement values were then used to develop predictive relationships for displacement as a function of a_y and different combinations of ground motion parameters (Peak Ground Acceleration, Peak Ground Velocity, Mean Period, Arias intensity), with the goal of identifying the combinations of ground motion parameters that produce the smallest variability in the prediction of sliding displacement.

2.2.3 Regional Prediction Models for Other Active Tectonic Regions

A regional empirical NSB displacement prediction model for Taiwan was proposed by Hsieh and Lee (2011) based mainly on strong motions recorded during 1999 Chi-Chi Earthquake (746 strong-motion records). In this study, global NSB displacement prediction models were also proposed using a subset of PEER NGA-W1 database. The parameters used in the prediction model were similar to the previous studies (Arias Intensity and critical acceleration) however, local site conditions were also considered and separate prediction models for rock and soil conditions were provided. The authors suggested the use of rock-site model in regional evaluation of the landslide hazard caused by earthquakes since most natural slope failures happen on hillsides, lay at the top of the bedrock. They recommended the soil site formula to be used for slopes of landfills.

Bozbey and Gündoğdu (2011) developed empirical NSB displacement prediction models by using a dataset compiled by Earthquake Department of General Directorate of Disaster Affairs (AFAD) with 50 strong-motions recorded during 37 earthquakes occurred in Turkey. The functional form of the model is similar to the model proposed by Jibson (2007).

NSB displacement prediction models introduced above are discussed elaborately in the following section in terms of their functional forms and compatibility with the ground motion dataset of Turkey.

CHAPTER 3

COMPATIBILITY OF NEWMARK SLIDING BLOCK DISPLACEMENT PREDICTIVE MODELS FOR TURKEY

Implementation of global ground motion prediction equations (GMPEs), especially the NGA-W1 models developed mainly for California in the other shallow crustal and active tectonic regions is a topic of ongoing discussion. To check the compatibility of the magnitude, distance, and site amplification scaling of NGA-W1 horizontal attenuation relationships with the ground motions that took place in Turkey, Gülerce et al. (2013) remodeled the lately developed TSMD (Akkar et al., 2010). Analysis results showed that the horizontal NGA-W1 models over predict the ground motions from the earthquakes occurred in Turkey, especially the small magnitude events recorded on stiff soil-rock sites. Therefore, any predictive model based on the global datasets may show a divergence from the regional ground motion characteristics and these global models should be evaluated before being implemented in probabilistic seismic hazard assessment (PSHA) studies in Turkey.

Within the contents of this chapter, predictions of NSB displacement models introduced in Chapter 2 are compared with the actual ground motion intensity measures and NSB displacement values in the comparison dataset of Turkey to find the most compatible model (or models). A brief summary of the Gülerce et al. (2013) dataset with the emphasis on NSB displacement values is provided at the beginning. Then, the general procedure for the analysis of model residuals is demonstrated in a stepwise manner. Compatibility of each model with the comparison dataset of Turkey is evaluated and presented individually in the subsequent sections, and finally, most appropriate NSB displacement model for the PSHA applications in Turkey is chosen. Application of the selected model in general PSHA framework will be presented in the next chapter.

3.1 COMPILATION OF THE COMPARISON DATASET

Strong motion data recorded by the Turkish national strong motion network had been gathered and analyzed together with detailed site measurements for recording stations by Akkar et al. (2010). The TSMD including 4067 sets of recordings from 2996 events occurred between years 1976-2007 is presented through the internet at http://daphne.deprem.gov.tr. Gülerce et al. (2013) used TSMD as a starting point for the regionalization of global NGA-W1 models for Turkey. An exhaustive review of the alterations on the initial database, the ways of predicting the unknown parameters required for comparison with the NGA-W1 attenuation models, determination of the orientation-independent intensity measures and the revised comparison dataset can be found in Gülerce et al. (2013), but a brief summary is given below:

- Only 173 earthquakes (approximately 6% of the total number of recorded events) were magnitude 5 or bigger and during these events 685 recordings were taken. To preserve all valuable data, all of these recordings were added to the comparison dataset.

- The recordings from small magnitude (M_w<5) events were added in the comparison dataset only if more than three recordings were available in the database.

- The moment magnitude values for 119 of earthquakes were unavailable, so they were predicted from local magnitude (M_L) with the help of recently proposed relationships by Ulusay et al. (2004) and Akkar et al. (2010).

- No site-specific detail (V_{S30} or any site classification) was able to be found for 431 remaining recordings. The V_{S30} values of 49 recordings were estimated from the NGA-W1 dataset and rest of the recordings were removed.

- The style of faulting for 47 events was estimated using the mechanisms of other earthquakes in the sequence or the dominant mechanism of the region.

- Most of the recordings in the remaining dataset were processed by Akkar et al. (2010). With the intention of preserving data as much as possible to acquire a representative dataset, 284 unfiltered recordings were included to the database along with processed data.

- Final comparison dataset consists of 1142 recordings derived from 288 events with the earthquake metadata, distance metrics for the recordings, V_{S30} values for the recording stations, and spectral accelerations of the horizontal and vertical component.

A yield acceleration (a_y) value should be defined in order to calculate the NSB displacements for the recordings in the comparison dataset. Jibson (1993) and Jibson et al. (1998) calculated the NSB displacement for several values of yield acceleration, ranging from 0.02g to 0.40g to produce a well-constrained dataset for the NSB displacement regression analysis. Similarly, Bray and Travasarou (2007) developed their model for the values of the yield coefficients between 0.02 and 0.4, and Hsieh and Lee (2011) computed the NSB displacements for yield accelerations between 0.01g and 0.4g. Watson-Lamprey and Abrahamson (2006) computed the NSB displacements for only three a_y values (0.1g, 0.2g and 0.3g), however they scaled the ground motions to create a bigger dataset for these higher a_y values. Saygılı and Rathje (2008) had chosen four a_y values (0.05g, 0.1g, 0.2g, and 0.3g) to encompass typical values for the earth slopes. Bozbey and Gündoğdu (2011) calculated the yield accelerations according to the a_y/a_{max} ratio; the a_{max} values defined from individual strong ground motion recordings was multiplied by ratios ranging from 0.01 to 1.0. Within the contents of this study, it was preferred not to scale the ground motions in the comparison dataset. Instead, the recommendations of Jibson et al. (1998) were followed and the NSB displacements were calculated for yield accelerations between 0.02g to 0.40g to develop a better constrained dataset. The selected values of yield accelerations in previous studies and for this study are summarized in Table 3.1. Calculated NSB displacements for each recording at each yield acceleration value are added to the comparison dataset.

Number of ground motion recordings in the final comparison dataset with PGA values bigger than the lowest yield acceleration given in Table 3.1 is limited to 220 for the horizontal components in N-S direction and 213 for the horizontal components in E-W direction. Both N-S and E-W components of 190 common recordings have PGA values over 0.02g, therefore, the total number of recordings giving non-zero NSB displacements in the Gülerce et al. (2013) dataset is 243 for the smallest yield acceleration value. The number of recordings in the comparison dataset decreases significantly with the increase in the yield acceleration value as shown in Figure 3.1. According to Figure 3.1, almost 80% of the strong ground motion recordings in the dataset have a PGA value less than 0.1g.

Table 3.1 Selected values of yield accelerations (a_y) in previous NSB predictive models and for this study.

Method	a_y values used (g)
Jibson (1993) Jibson et. al (1998)	0.02, 0.05, 0.10, 0.20, 0.30 and 0.40
Jibson (2007)	0.05, 0.10, 0.20, 0.30 and 0.40
Watson-Lamprey and Abrahamson (2006)	0.10, 0.20 and 0.30
Bray and Travasarou (2007)	0.02, 0.05, 0.075, 0.10, 0.15, 0.20, 0.25, 0.30, 0.35 and 0.40
Saygılı and Rathje (2008)	0.05, 0.10, 0.20 and 0.30
Hsieh & Lee (2011)	0.01, 0.02, 0.05, 0.10, 0.20, 0.25, 0.30, 0.35 and 0.40
Bozbey and Gündoğdu (2011)	0.01*a_{max}, 0.05*a_{max}, 0.10*a_{max}, 0.20*a_{max}, 0.30*a_{max}, 0.40*a_{max}, 0.50*a_{max}, 0.60*a_{max}, 0.70*a_{max}, 0.80*a_{max}, 0.90*a_{max} and 1.0*a_{max}
This study	**0.02, 0.05, 0.10, 0.20, 0.30 and 0.40**

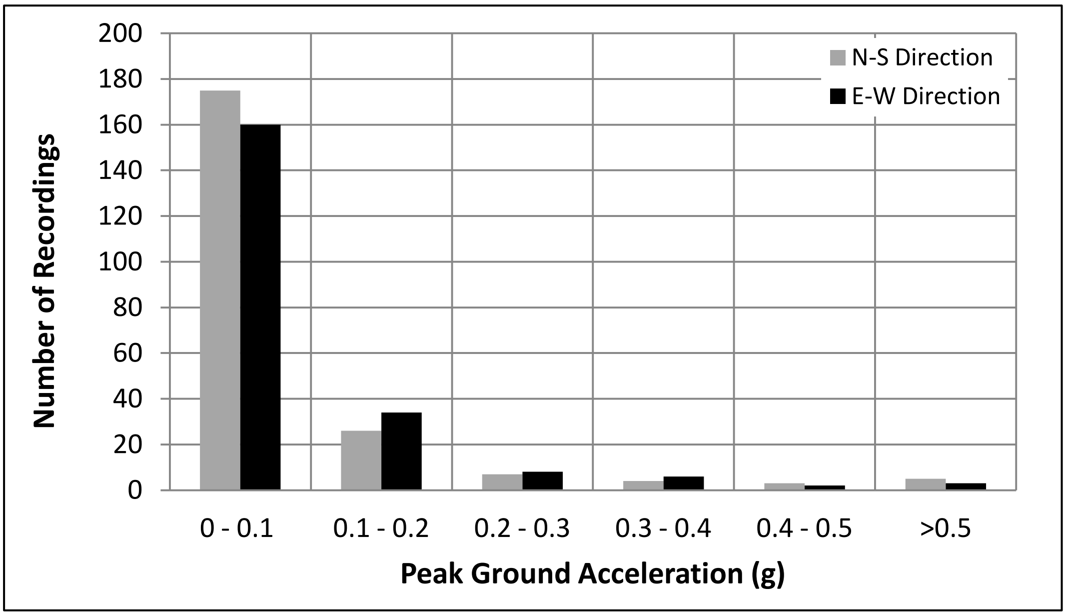

Figure 3.1 Peak ground acceleration (a_{max}) range distribution of the used ground motion records for both directions

Statistics of the recordings remained in the comparison dataset (recordings with NSB displacement>0 for the smallest yield acceleration) is introduced through Figures 3.2-3.4 to put forth the reliability and the limitations of the dataset to assess the NSB displacement predictive models. Figure 3.2 shows the magnitude-distance distribution of the recordings and Figure 3.3 presents the number of recordings in each magnitude bin among the comparison dataset. As Figures 3.2 and 3.3 imply, the recordings obtained from events with magnitudes between 6.0 and 7.0 and recordings from the moderate-to-large magnitude events within 30 kilometer from the rupture are rather sparse. Almost half of the strong ground motion records included in the dataset have a moment magnitude value in between 4.5 and 5.5. Moreover, 1999 Kocaeli and Düzce earthquakes are the only events in the dataset with magnitude greater than 7.0. This characteristic of the dataset is not the consequence of the excluded data points, same fact was also pointed out by Akkar et al. (2010) for the TSMD database. The number of recordings in various V_{S30} bins is presented in Figure 3.4. This figure shows that most of the strong ground motion recordings included in the dataset were obtained from stiff soil and soft rock sites according to NEHRP site classification.

Figures 3.2-3.4 suggests that the comparison dataset is relatively larger than the dataset of the only regional model (Bozbey and Gündoğdu, 2011). However, it is significantly smaller than the dataset of NGA-W1 dataset based models, especially in the moderate-to-large magnitude range.

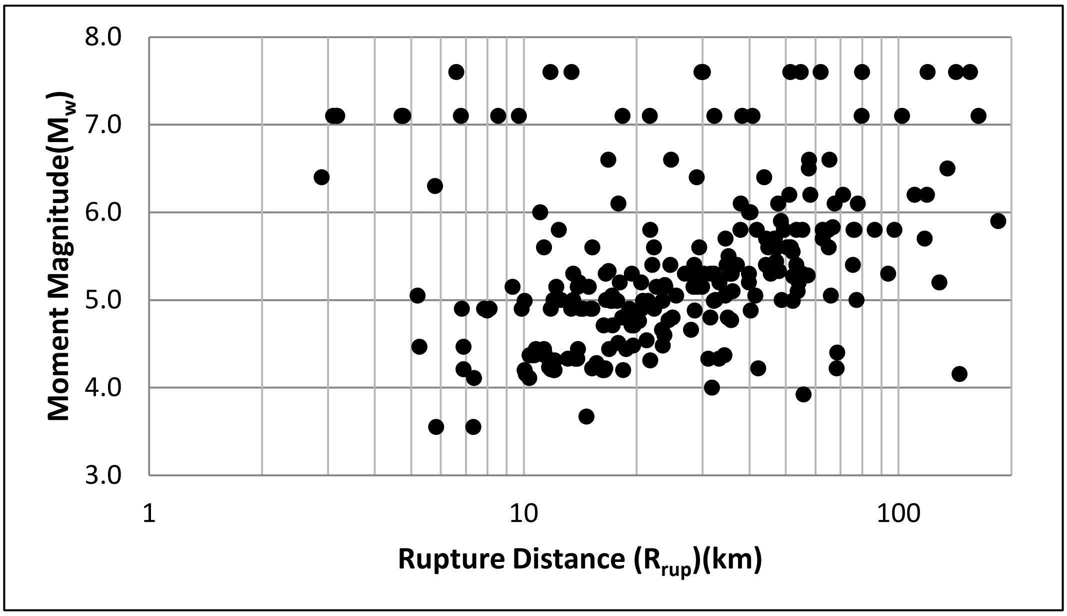

Figure 3.2 Magnitude-distance distribution of recordings in the comparison dataset for the smallest yield acceleration value.

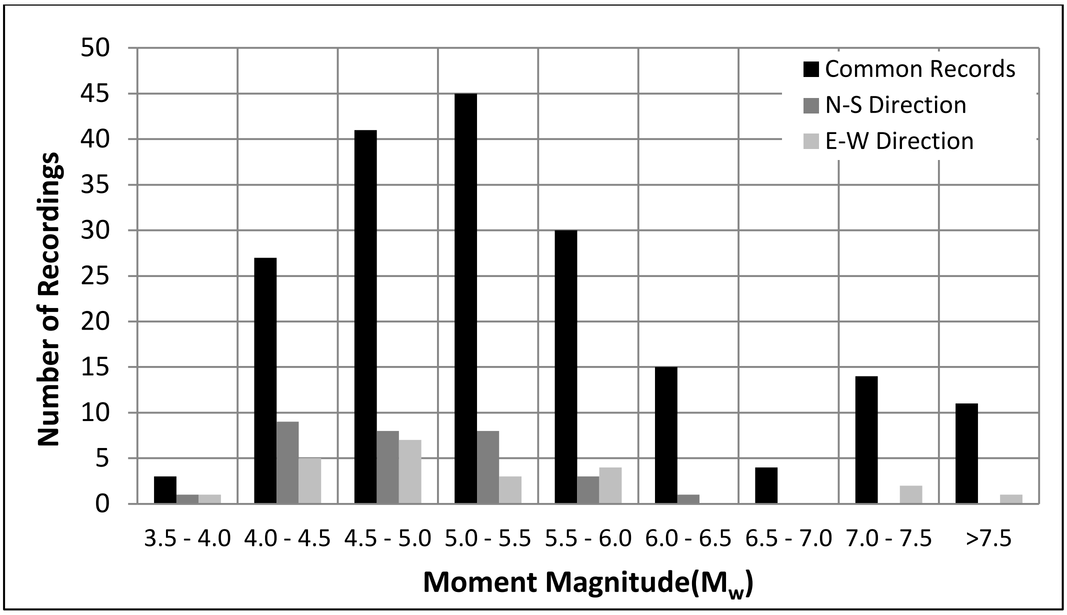

Figure 3.3 Magnitude (M_w) range distribution of the ground motion recordings in the comparison dataset for the smallest yield acceleration value.

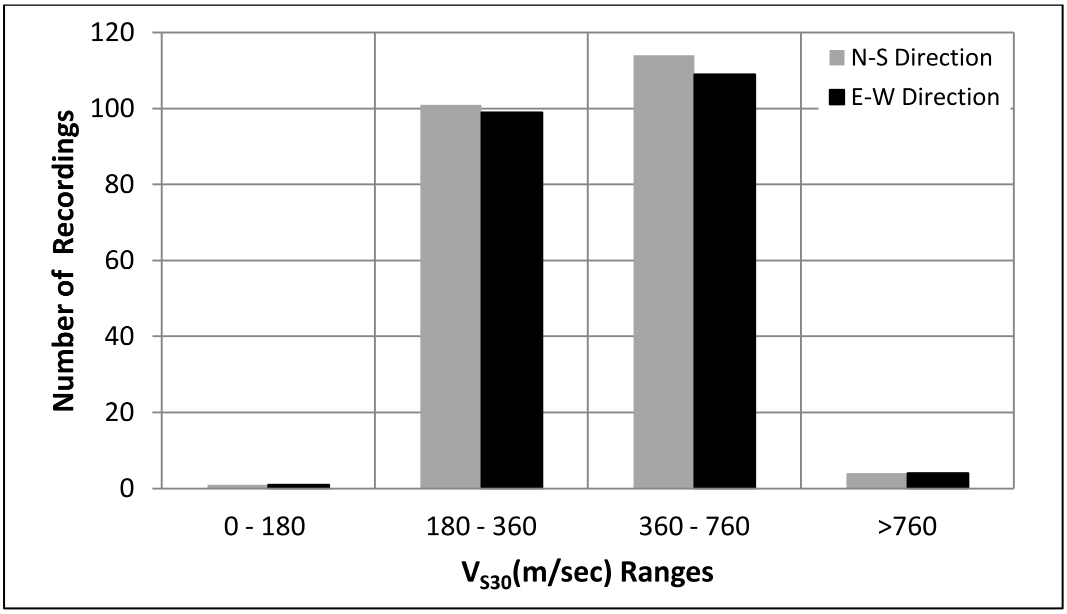

Figure 3.4 Shear wave velocity (V_{s30}) (m/sec) range distribution of the ground motion records in the comparison dataset for the smallest yield acceleration value (0.02g).

3.2 METHODOLOGY: ANALYSIS OF MODEL RESIDUALS

To evaluate the differences between the model predictions and the actual data is the analysis; the model of residuals method is preferred. Following procedure is applied:

- The ground motion parameters in the NSB displacement predictive models mentioned in Chapter 2 are tabulated in Table 3.2. A MATLAB routine is constructed to calculate the parameters listed in Table 3.2 for each ground motion in the dataset. These parameters are added to the comparison dataset flat file.

- NSB displacements for the given yield acceleration are calculated for both N-S and E-W direction horizontal components of each ground motion in the dataset using the same MATLAB routine. For each horizontal component, displacements are calculated for both positive and negative polarities (by flipping the time history upside down), and the largest displacement is assigned as the NSB displacement for that horizontal component. Therefore, each ground motion has two different NSB displacements in the flatfile for each yield acceleration value.

- Some of the NSB prediction studies proposed more than one alternative model with different parameters for different site conditions or different tectonic characteristics (global or regional databases). The equations, which are derived from global datasets and developed for rock site conditions, are selected as representative model for each study. Details of this selection process are also provided separately in the next section.

Table 3.2 Ground motion parameters included in the evaluated NSB displacement predictive models.

<table>
<tr><th>NSB Predictive Model</th><th>Included Parameters</th></tr>
<tr><td rowspan="4">Watson-Lamprey and Abrahamson (2006)</td><td>Spectral Acceleration at T= 1 sec. ($Sa_{T=1s}$)</td></tr>
<tr><td>Acceleration Root Mean Square (A_{RMS})</td></tr>
<tr><td>Peak Ground Acceleration (PGA)</td></tr>
<tr><td>Duration for which the acceleration is greater than the yield acceleration (Dur_{ky})</td></tr>
<tr><td>Jibson (2007)</td><td>Arias Intensity (I_a)</td></tr>
<tr><td rowspan="2">Bray and Travasarou (2007)</td><td>Peak Ground Acceleration (PGA)</td></tr>
<tr><td>Moment Magnitude (M_w)</td></tr>
<tr><td rowspan="3">Saygılı and Rathje (2008)</td><td>Peak Ground Acceleration (PGA)</td></tr>
<tr><td>Peak Ground Velocity (PGV)</td></tr>
<tr><td>Arias Intensity (I_a)</td></tr>
<tr><td>Bozbey and Gündoğdu (2011)</td><td>Maximum Acceleration (a_{max})</td></tr>
<tr><td>Hsieh & Lee (2011)</td><td>Arias Intensity (I_a)</td></tr>
</table>

- NSB displacement model predictions for each recording in the comparison dataset for each candidate model and each yield acceleration value is determined and the total model residual is calculated using Equation 3.1 or 3.2 as given below:

  $$Residual = ln(actual) - ln(predicted) \qquad \mathbf{3.1}$$

  $$Residual = log(actual) - log(predicted) \qquad \mathbf{3.2}$$

  where ln(actual) and log(actual) is the NSB displacement for one of the horizontal components of the recording and ln(predicted) and log(predicted) is the model prediction in natural log terms or log terms.

- Plots of the total residuals with respect to the ground motion parameters included in each predictive model as well as the other ground motion parameters listed in Table 3.2 are prepared to evaluate the differences between the NSB displacement comparison dataset of Turkey and the model predictions.

- A model is considered to be applicable for the probabilistic NSB displacement hazard analysis studies to be conducted in Turkey if: (i) there is no trend observed in the total residual plots for any ground motion parameter or (ii) there is only a constant shift in the total residuals along the zero line which can be easily fixed by changing the constant term of the equation.

3.3 COMPATIBILITY OF THE PREDICTIVE MODELS

Details of the alternative models proposed in each study and evaluation results for each model are provided individually in each subsection below.

3.3.1 Watson-Lamprey and Abrahamson (2006)

In many seismic analyses, beside the design response spectrum are also required for dynamic analyses. Generally, the acceleration-time histories are selected within the recorded ground motions with similar magnitudes and similar distances with the design earthquake. Some other factors like the site condition, faulting style, and spectral content may also be taken into account. According to Watson-Lamprey and Abrahamson (2006), besides these factors, the scale factor can also be taken into account as an important factor in acceleration-time histories selection. They proposed a method for selecting time series such that after scaling, selected time series will lead to a near average response of a non-linear system. The method requires defining a simple non-linear model that can serve as a proxy for a more complicated non-linear model, and then using the simple non linear model to find the time series that lead to an average response of the simple model.

The NSB method is used as the simple non linear proxy by Watson-Lamprey and Abrahamson (2006). The PEER NGA-W1 strong motion database containing 6158 records (both N-S and E-W components) from 175 earthquakes was used for this study. The average values for PGV, PGA and Arias Intensity were determined for the whole database and the individual recordings were then scaled to match each of these average values (PGA= 0.44g, PGV= 50 cm/s, Arias Intensity= 0.18 g^2s). The NSB displacements were calculated for a_y= 0.1g. To evaluate the limits for which the scaling is valid, the resulting displacements are plotted against the scale factor. For all three scaling parameters, the displacement is found to be correlated with the scale factor. This indicates that the computed displacement will be biased if large (or small) scale factors are used.

Then, by carrying out a regression analysis model for the NSB displacement based solely on characteristics of the ground motion time series was developed. The 6158 strong-motion records from the data set were scaled by different scale factors of 0.5, 1, 2, 4, 8, 16 and 20. The NSB displacements of these scaled recordings were then computed for yield accelerations of 0.1, 0.2 and 0.3g. Therefore, totally 129,318 displacements were obtained. Then, these displacements were fit to the Equation 3.3 by using least squares regression:

$$\begin{aligned}\ln(Newmark\ Disp(cm))\\ = \Bigg(5.470 + 0.451(ln(Sa_{T=1s}) - 0.45) + 0.0186(ln(Sa_{T=1s}) - 0.45)^2\\ + 0.596(ln(A_{RMS}) - 1) + 0.656\left(ln\left(\frac{Sa_{T=1s}}{PGA}\right)\right) + (-0.716)\left(ln\left(\frac{Sa_{T=1s}}{PGA}\right)\right)^2\\ + 0.802\big(ln(Dur_{ky}) - 0.74\big) + 0.0763\big(ln(Dur_{ky}) - 0.74\big)^2\\ + 1/(-0.581)\left(ln\left(\frac{PGA}{ky}\right) + 0.193\right)\Bigg) \qquad \mathbf{3.3}\end{aligned}$$

where $\mathrm{Sa_{T=1s}}$ is spectral acceleration with 5% damping at 1 second spectral period in g, PGA is the peak ground acceleration in g, $\mathrm{A_{RMS}}$ is the acceleration root mean square in g, $\mathrm{k_y}$ is the yield acceleration in g, and the $\mathrm{Dur_{ky}}$ is the duration for which the acceleration is greater than the yield acceleration in seconds. The estimated coefficients and standard errors are presented in the study however; a total standard deviation for the predictive model was not provided.

The performance of the NSB displacement predictive model given in Equation 3.3 on the comparison dataset of Turkey is evaluated using the total residual plots for with respect to several ground motion parameters: PGA/k_y, Arias intensity, PGA, PGV, $Sa_{T=1s}$, $Sa_{T=1s}$/PGA, A_{RMS} and duration through Figure 3.5(a) to Figure 3.5(h), respectively. No trend in the residuals are observed in Figure 3.5(a), Figure 3.5(b), Figure 3.5(c), Figure 3.5(d), and Figure 3.5(g).

However, a constant shift along the zero line is visible in all of these plots indicating that the constant term of the model (5.47 in Equation 3.3) should be modified for the dataset of Turkey. Figures 3.5(e) and 3.5(f) imply that the prediction model miscalculates the actual data, especially for the small spectral accelerations. This result is expected since the NGA-W1 models for the horizontal ground motion component significantly overestimated the ground motions in the same comparison dataset (especially for small-to-moderate magnitudes) and those features of the NGA-W1 models had to be adjusted (Gülerce et al., 2013). A similar adjustment may be applied to this method, however, the dataset used in this study is quite small (only 243 ground motions) therefore the results may not be very reliable. A similar trend in the residuals is observed in the duration plot (Figure 3.5(h)) which is related to the differences in the definition of duration in Watson-Lamprey and Abrahamson (2006) and this study (according to the definition for the duration term in Equation 3.3; Dur_{ky} is assumed to be the bracketed duration).

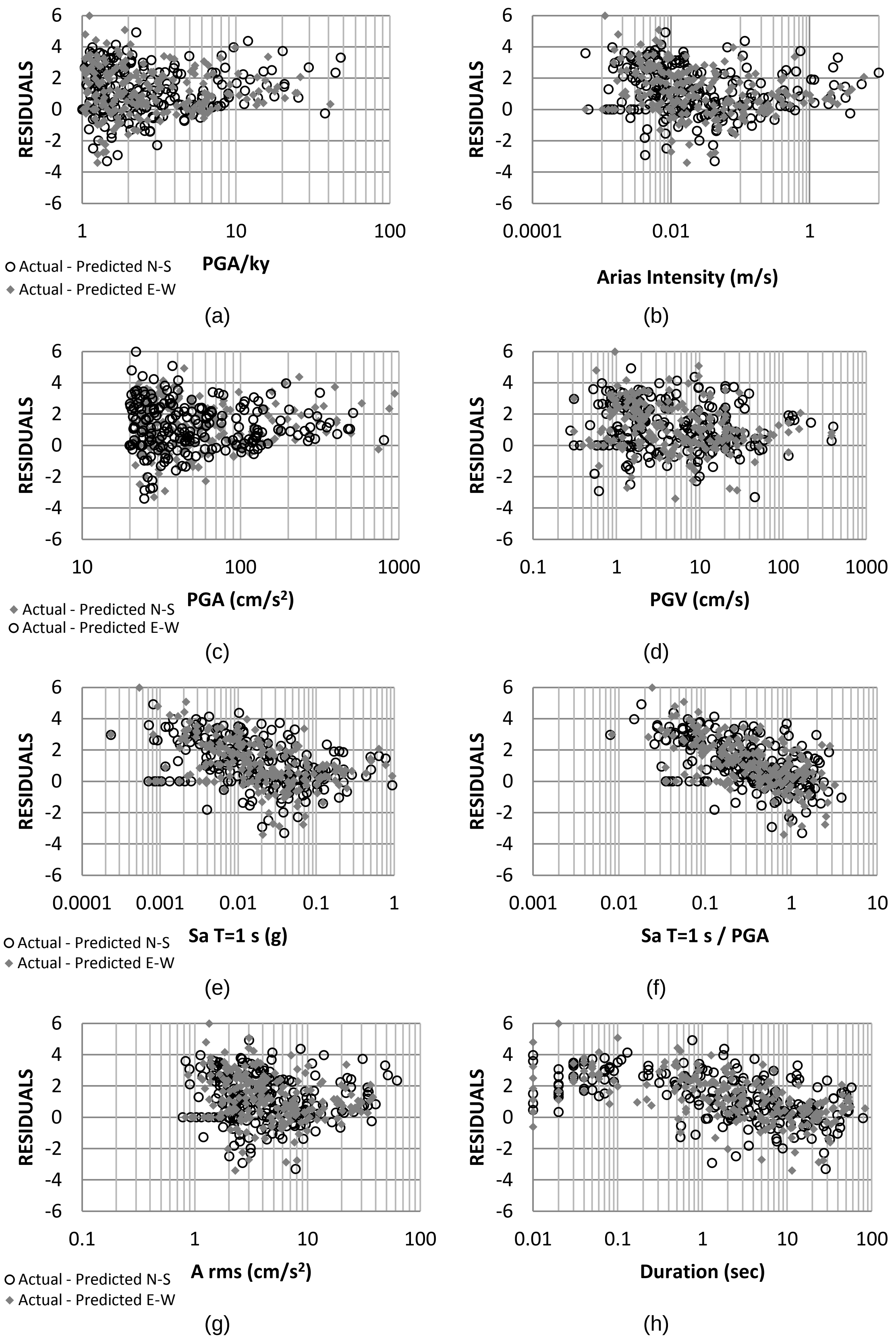

Figure 3.5 Residuals vs. a) PGA/k_y, b) Arias Intensity, c) PGA, d) PGV, e) S_a T=1s, f) S_a T=1s/PGA, g) A_{rms} and h) Duration at k_y=0.02g for Watson-Lamprey & Abrahamson (2006)

3.3.2 Jibson (2007)

First studies of developing simple regression models to estimate NSB displacement were based on the analysis by using the limited number of strong-motion records then available records. The current availability of a much larger dataset of records causes the renewal of these regression models, so the recent NSB prediction model proposed by Jibson (2007) is selected as the representative model for all the other models proposed by Jibson and his co-workers (Jibson (1993), Jibson et. al (1998) and Jibson (2007)). Jibson (2007) built the NSB displacement prediction model using the data of 2270 strong-motion records derived from 30 earthquakes. To produce a well-constrained dataset, NSB displacements were calculated for a_c (definition is same as a_y) values of 0.05g, 0.10g, 0.20g, 0.30g, and 0.40g. A variety of regression models of different forms with different ground motion variables were proposed as given in Equations 3.4 to 3.7:

$$\log \mathrm{D_n} = 0.215 + \log\left[\left(1-\frac{\mathrm{a_c}}{\mathrm{a_{max}}}\right)^{2.341}\left(\frac{\mathrm{a_c}}{\mathrm{a_{max}}}\right)^{-1.438}\right] \pm 0.510 \qquad \mathbf{3.4}$$

$$\log \mathrm{D_n} = -\,2.710 + \log\left[\left(1-\frac{\mathrm{a_c}}{\mathrm{a_{max}}}\right)^{2.335}\left(\frac{\mathrm{a_c}}{\mathrm{a_{max}}}\right)^{-1.478}\right] + 0.424\mathrm{M} \pm 0.454 \qquad \mathbf{3.5}$$

$$\log \mathrm{D_n} = 2.401 \log \mathrm{I_a} - 3.481 \log \mathrm{a_c} - 3.230 \pm 0.656 \qquad \mathbf{3.6}$$

$$\log \mathrm{D_n} = 0.561 \log \mathrm{I_a} - 3.833 \log(\mathrm{a_c}/\mathrm{a_{max}}) - 1.474 \pm 0.616 \qquad \mathbf{3.7}$$

where $\mathrm{D_n}$ is the NSB displacement in centimeters, $\mathrm{a_c}$ is the critical (or yield) acceleration in g, $\mathrm{a_{max}}$ (or PGA) is the maximum acceleration in g, M is the moment magnitude, and $\mathrm{I_a}$ is Arias intensity in meters per second. The last term in each equation stands for the standard deviation of the model.

Equations 3.4 and 3.5 have higher R^2 values (0.87 and 0.84 respectively) than the other two equations (R^2= 0.71 for Equation 3.6 and R^2= 0.75 for Equation 3.7) which increases the statistical stability of these equations. However, Jibson (2007) mentions that the Arias intensity is predominant to PGA in characterizing the intensity of a strong-motion record since it takes into consideration of all acceleration peaks and for duration, therefore Equations 3.6 and 3.7 are physically stronger. In Equation 3.7, the R^2 value improves to 0.75 and the standard deviation value decreases slightly. On the other hand, a sampling had to be applied to the dataset due to the maximum acceleration limit for this functional form. Therefore, Equation 3.6 is chosen to be the representative prediction equation for this study.

The performance of the NSB displacement predictive model given in Equation 3.6 on the comparison dataset of Turkey is evaluated using the total residual plots for with respect to several ground motion parameters: Arias intensity, PGA, PGV, A_{RMS} and duration in Figure 3.6(a) to Figure 3.6(e), respectively. Significant trends along the zero line are observed in all of these plots, except for the PGV in Figure 3.6(c), which is found to be a less sensitive parameter to the regional ground motion characteristics. Figure 3.6(a) indicates that the variables in Equation 3.6, especially the variable related to Arias intensity, should be modified. Figures 3.6(b), 3.6(d), and 3.6(e) imply that performance of the prediction model would be improved if more ground motion intensity measures like A_{RMS} and PGA were included.

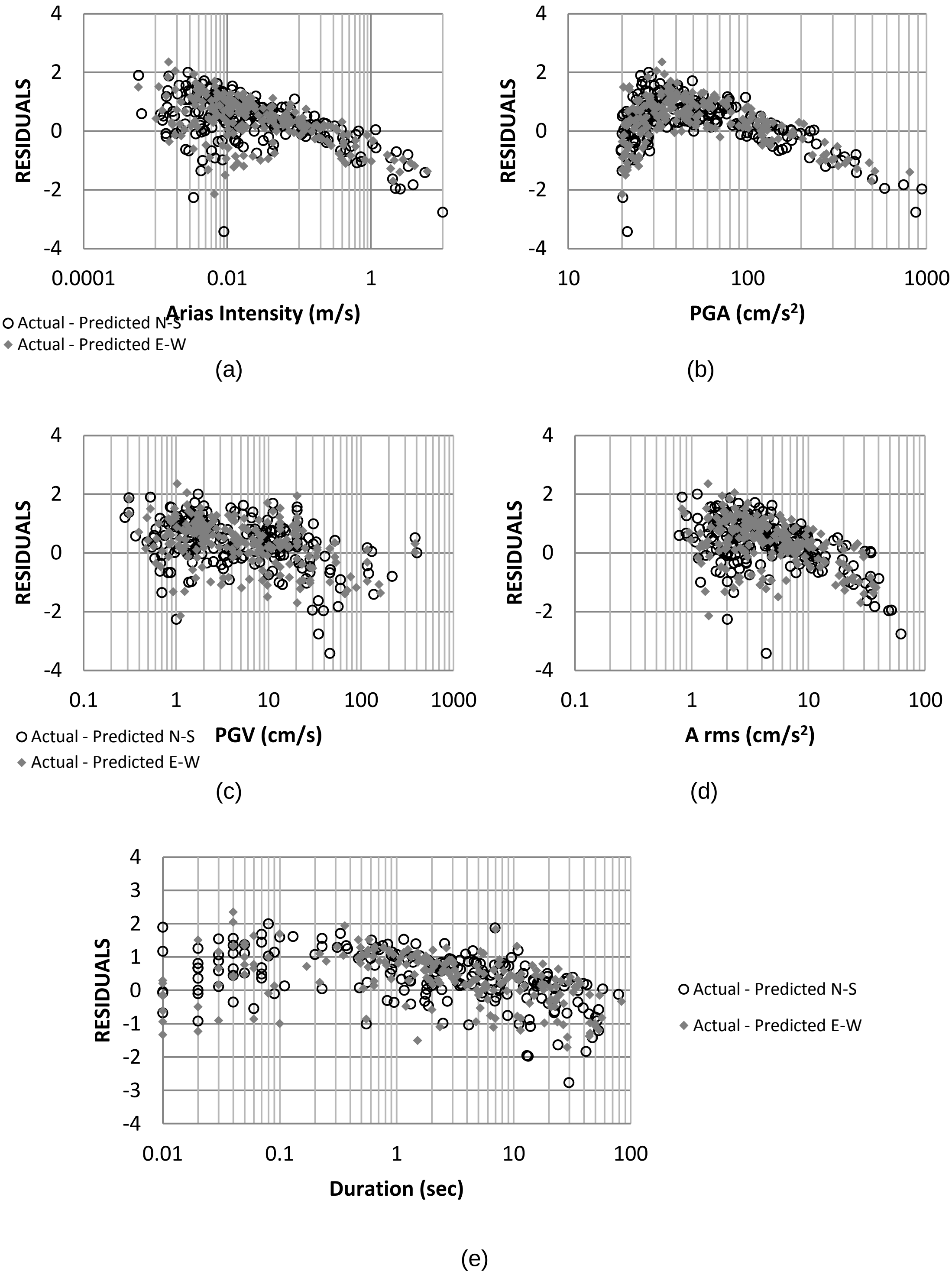

Figure 3.6 Residuals vs. a) Arias Intensity, b) PGA and, c) PGV, d) A_{rms} and e) Duration at k_y=0.02g for Jibson (2007)

3.3.3 Bray and Travasarou (2007)

The main objective of Bray and Travasarou (2007) was to describe a simplified semi-empirical procedure that can be used in the assessment of the likely performance of earth/waste structures that may slide during earthquakes. The procedure was developed to work within a fully probabilistic seismic hazard assessment, but it can be used also as a simple predictive relationship that includes quantification of the uncertainty of key input variables.

Non-linear, coupled, stick-slip deformable sliding mass model with one-way sliding was used in the study. According to Bray and Travasarou (2007), top of a slope can move downward due to either deviatoric deformation or volumetric compression of the material that composes the slope. However, top of slope movements resulting from distributed deviatoric straining within the sliding mass or stick-slip sliding along a failure surface have a different mechanism than the top of slope movements that result from seismically induced volumetric compression of the materials forming the slope. The Newmark sliding block method provides a simplified analogy to explain the deviatoric deformation. There are cases where the NSB analogy does not capture the overall top of slope displacement, such as the seismic compression of large compacted earth fills. Hence, the authors preferred to separate these effects and use procedures based on the sliding block model to estimate deviatoric-induced displacements only. Procedures based on the seismic compression of soils were recommended to estimate volumetric-induced displacements (Bray and Travasarou, 2007).

The sliding mass was assigned a constant unit weight of 17.6 kN/m^3, and model was characterized by: (1) by its yield coefficient a_y, the strength, and (2) by its initial fundamental period T_s, which represents dynamic stiffness. After evaluating some cases, it was found that the spectral acceleration at a degraded period equal to 1.5 times the initial fundamental period of the slope [$S_a(1.5T_s)$] was overall the most efficient intensity measure. This degraded fundamental period captures the overall average stiffness reduction for the earth/waste slopes considered in the study. Hence, the recommended equation for predicting the seismic displacement amount (D) is:

$$\begin{aligned} ln(D) = -1.10 - 2.83 ln(k_y) - 0.333\left(ln(k_y)\right)^2 + \ 0.566\ ln(k_y) ln(S_a(1.5T_s)) \\ + 3.04 ln(S_a(1.5T_s)) - 0.244\left(ln(S_a(1.5T_s))\right)^2 + 1.50T_s + 0.278(M-7) \pm \epsilon \quad \mathbf{3.8} \end{aligned}$$

where k_y is the yield coefficient, T_s, is the initial fundamental period of the sliding mass in seconds, and $S_a(1.5T_s)$is the spectral acceleration of the input ground motion at a period of $1.5T_s$ in the units of g, M is the moment magnitude and ε is a normally distributed random variable with zero mean and standard deviation of σ= 0.66.

After determining Equation 3.8, Bray and Travasarou (2007) plotted the residuals of the model versus some of the key independent ground motion intensity measures. A moderate trend was observed in the residual plots with respect to PGA and spectral accelerations at T_s= 2 s. Since it is uncommon in earth/waste sliding masses of periods greater than 1.5 seconds, the overestimation at 2 seconds was not significant. On the other hand, the equation was unconservative for the rigid body case (where T_s= 0) for very shallow slides. To eliminate the bias in the model when $T_s \approx 0$ s, the first term (-1.10) should be replaced with −0.22 when Ts<0.05 s. Because the standard deviation of Equation 3.8 is 0.66 and exp(0.66) ≈ 2, the median minus one sigma to median plus one sigma range of NSB displacement can be approximately estimated as half of the median estimate to twice of the median estimate of seismic displacement. Hence, the median seismic displacement calculated using the equation with ε= 0 can be halved and doubled to develop approximately the 16% to 84% exceedance seismic displacement range estimate.

Therefore, the equation modified into:

$$\ln(\mathrm{D}) = -0.22 - 2.83\ln(\mathrm{k_y}) - 0.333\left(\ln(\mathrm{k_y})\right)^2 + 0.566\ln(\mathrm{k_y})\ln(\mathrm{PGA}) + 3.04\ln(\mathrm{PGA}) - 0.244\left(\ln(\mathrm{PGA})\right)^2 + 0.278(\mathrm{M}-7) \pm \epsilon \qquad \mathbf{3.9}$$

where $\mathrm{k_y}$ is the yield coefficient, PGA is the peak ground acceleration in the units of g which is taking the place of $S_a(1.5T_s)$, M is the moment magnitude, and ε is the epsilon value defined above.

In order to evaluate the performance of the proposed model to predict the actual data in the ground motion dataset of Turkey, total residual plots with respect to the following ground motion parameters were investigated: Arias intensity, PGA, PGV, A_{RMS}, $Sa_{T=1s}$, duration and M_w through Figure 3.7(a) to Figure 3.7(g), respectively. Similar to the Jibson (2007) model, significant trends were observed in all of these plots revealing that the model is biased extensively, especially for the small magnitude and small ground shaking levels. Figures 3.7(b) and 3.7(g) indicate that the model variables given in Equation 3.9 should be revised for applicability in Turkey. Additionally, Figures 3.7(a), 3.7(d) and 3.7(f) imply that the model is unable to capture the ground motion properties represented by the Arias intensity, duration or A_{RMS} and any one of those parameters should be included in the predictive model.

It is also noteworthy that a part of this misfit comes from the recommended cutoff value for the application of the model. The authors mentioned that when the median NSB displacement is less than 1 cm the model assumes the displacement to be considered equal to zero for practical purposes since displacements smaller than 1 cm are considered not to be significant enough.

3.3.4 Saygılı and Rathje (2008)

Following the context of performance-based earthquake engineering, NSB displacement can be considered an engineering demand parameter that describes the performance of slopes. In the PSHA framework, the NSB displacement (D) can be computed as a function of test displacement levels, with the result being a NSB hazard curve that describes the annual rate of exceedance. The hazard integral for NSB displacement hazard curve would be similar to the traditional hazard integral, if only one ground motion intensity measure (IM) is employed by the NSB displacement prediction model. In this study, scalar PSHA (with one IM) is extended to a vector-valued PSHA that includes multiple characteristics of the ground motion to develop rigid block displacement predictive equations as given:

$$\lambda_D(x) = \sum_{z_i}\sum_{y_j} \times P\left[D > x \mid GM1 = z_i, GM2 = y_j\right] P\left[GM1 = z_i, GM2 = y_j\right] \qquad \mathbf{3.10}$$

In Equation 3.10, the NSB displacement is conditioned on two ground motion parameters, GM1 and GM2, and their joint probability of occurrence at two ground motion test levels GM1= z_i and GM2= y_j, P[GM1= z_i ,GM2= y_j]. Depending on the number of IMs included, the hazard integral should be modified and the correlation of the IMs should be included into the integration procedure.

Saygılı and Rathje (2008) proposed a generalized predictive model as:

$$\ln(\mathrm{D}) = -0.74 + (-4.93)\left(\frac{\mathrm{k_y}}{\mathrm{PGA}}\right) + (-19.91)\left(\frac{\mathrm{k_y}}{\mathrm{PGA}}\right)^2 + 43.75\left(\frac{\mathrm{k_y}}{\mathrm{PGA}}\right)^3 + (-30.12)\left(\frac{\mathrm{k_y}}{\mathrm{PGA}}\right)^4 + (-1.3)\ln(\mathrm{PGA}) + 1.04\ln(\mathrm{GM2}) + 0.67\ln(\mathrm{GM3}) \pm \epsilon\sigma_{\mathrm{lnD}} \qquad \mathbf{3.11}$$

where $\mathrm{k_y}$ is the yield coefficient, PGA is the peak ground acceleration in g, $\mathrm{GM2}$ and $\mathrm{GM3}$ are the ground motion parameters included in addition to PGA. For the scalar model, both GM terms were not utilized and for the 2 IM models, the GM3 term was cancelled. σ_{lnD} is the standard deviation in natural log units and ϵ is the standard normal variate with zero mean and unit standard deviation.

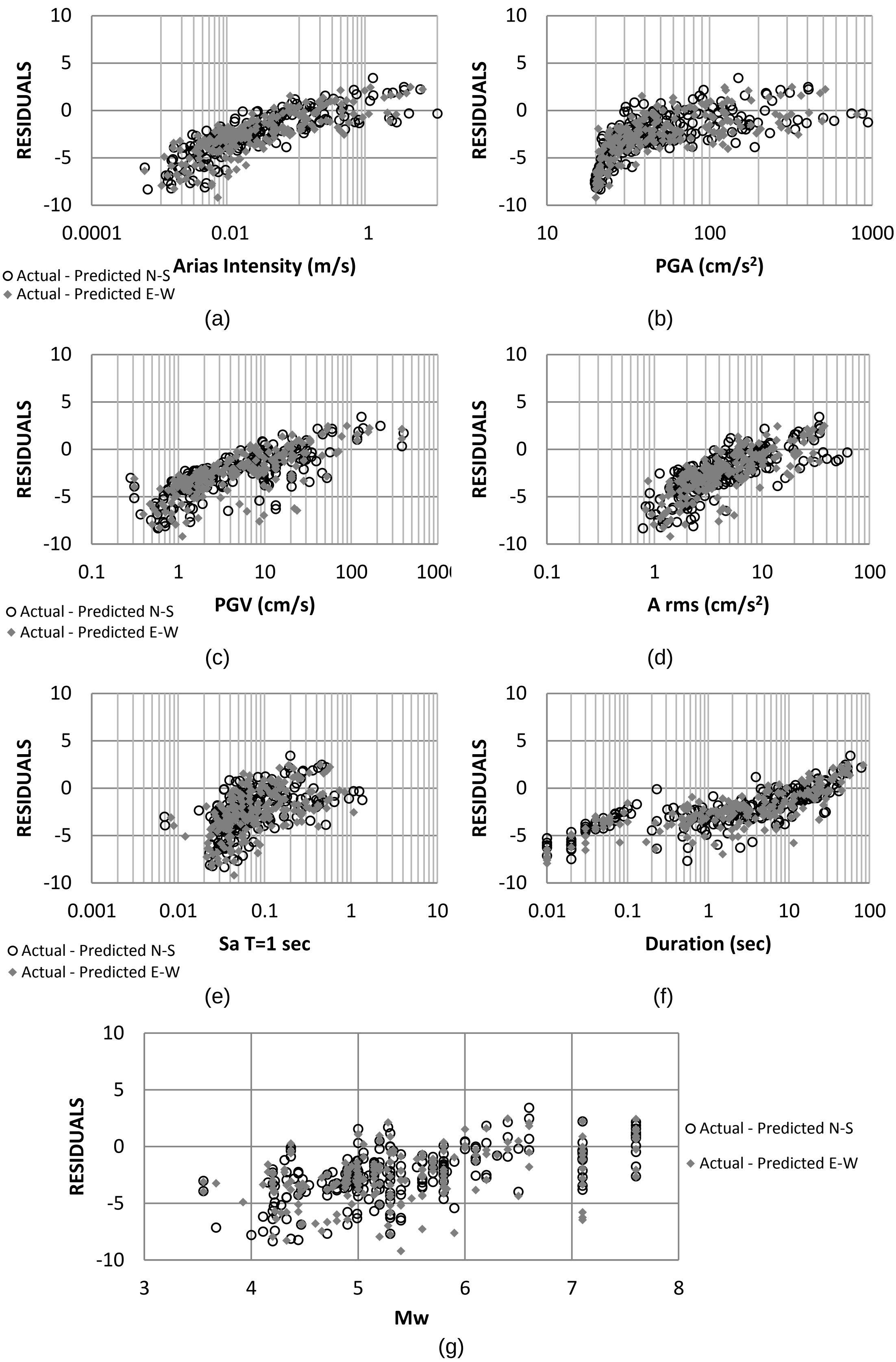

Figure 3.7 Residuals vs. a) Arias Intensity, b) PGA, c) PGV, d) A_{rms}, e) S_a T=1s, f) Duration and g) M_w at k_y=0.02g for Bray and Travasarou (2007)

Optimal ground motion parameters were selected among candidate IMs: peak ground acceleration (PGA), peak ground velocity (PGV), mean period (T_m), Arias intensity (I_a), and two definitions of duration based on the build-up of Arias Intensity [$D_{5–95}$ and $D_{5–75}$] by employing predominantly the "efficiency" criterion proposed by Cornell and Luco (2001). The term efficiency is related to the variability of the random error obtained from the regression. In this sense, the IM that produces less variability (σ_{ln}) in the NSB displacement prediction model are considered to be more efficient. When compared to the scalar model using only one IM (PGA), vector-valued models using two IMs result in a 40–60% reduction in the standard deviation. The duration parameters $D_{5–75}$ and $D_{5–95}$ do not significantly reduce σ_{lnD}. The three parameter vector models (PGA, PGV, I_a and PGA, T_m, I_a) further reduce σ_{lnD} by 15–40% at smaller values of k_y/PGA.

Cornell and Luco (2001) also specify a "sufficiency" criterion for predictive equations of engineering demand parameters, such that the selected ground motions can sufficiently predict the engineering demand parameter without the need for specifying the earthquake magnitude or site-to-source distance. The multi-parameter models which were described in the study also found to be more sufficient in predicting displacements over a range of earthquake magnitudes. Based on their ability to significantly reduce σ_{lnD} for the NSB displacement prediction, the two IM vector-valued model (PGA, PGV) and the three IM vector-valued model (PGA, PGV, I_a) were recommended by the authors.

Both two IM vector-valued model (PGA, PGV) and the three IM vector-valued model (PGA, PGV, I_a) is considered as candidate models for the PSHA applications in Turkey and their performance on predicting the actual data in the comparison dataset of Turkey are evaluated using the total residual plots. Total residual plots of the two IM vector-valued model (PGA, PGV) with respect to several ground motion parameters: Arias intensity, PGA, PGV, A_{RMS}, k_y/PGA and duration are presented in Figure 3.8(a) to Figure 3.8(f), respectively. No obvious trend in the residuals is observed in Figure 3.8(a-f), except for a slight over prediction observed in the total residuals for higher PGV values in Figure 3.8(c). However, a constant shift along the zero line is visible in all of these plots indicating that the constant term of the model (-0.74 in Equation 3.11) should be modified for the Turkish dataset.

Same plots are presented in Figure 3.9 for the three IM vector-valued model (PGA, PGV, I_a) with respect to the same ground motion parameters: Arias intensity, PGA, PGV, A_{RMS}, k_y/PGA and duration in Figures 3.9(a) to Figure 3.9(f), respectively. When compared to Figure 3.8, Figure 3.9 indicates that the inclusion of the third IM improved the performance of the model. No obvious trends in the residuals are observed in Figure 3.9(a) to Figure 3.9(f) and this time there is no constant shift along the zero line. Therefore, three IM vector-valued model (PGA, PGV, I_a) is preferable for PSHA applications in Turkey, even though it increases the computing time significantly.

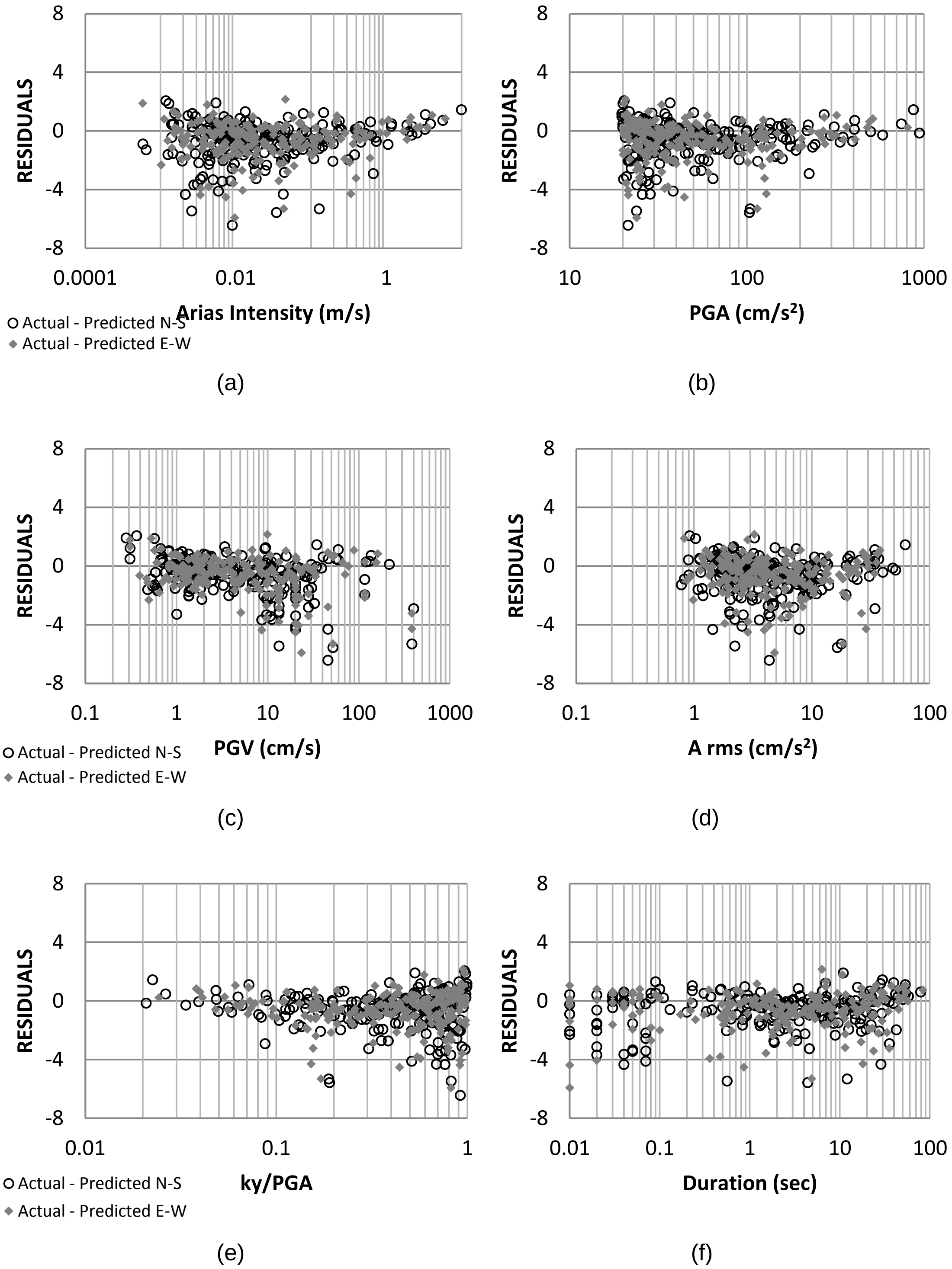

Figure 3.8 Residuals vs a) Arias Intensity, b) PGA, c) PGV, d) A_{rms}, e) k_y/PGA and f) Duration at k_y=0.02g of two parameter vector model (PGA, PGV) of Saygılı and Rathje (2008)

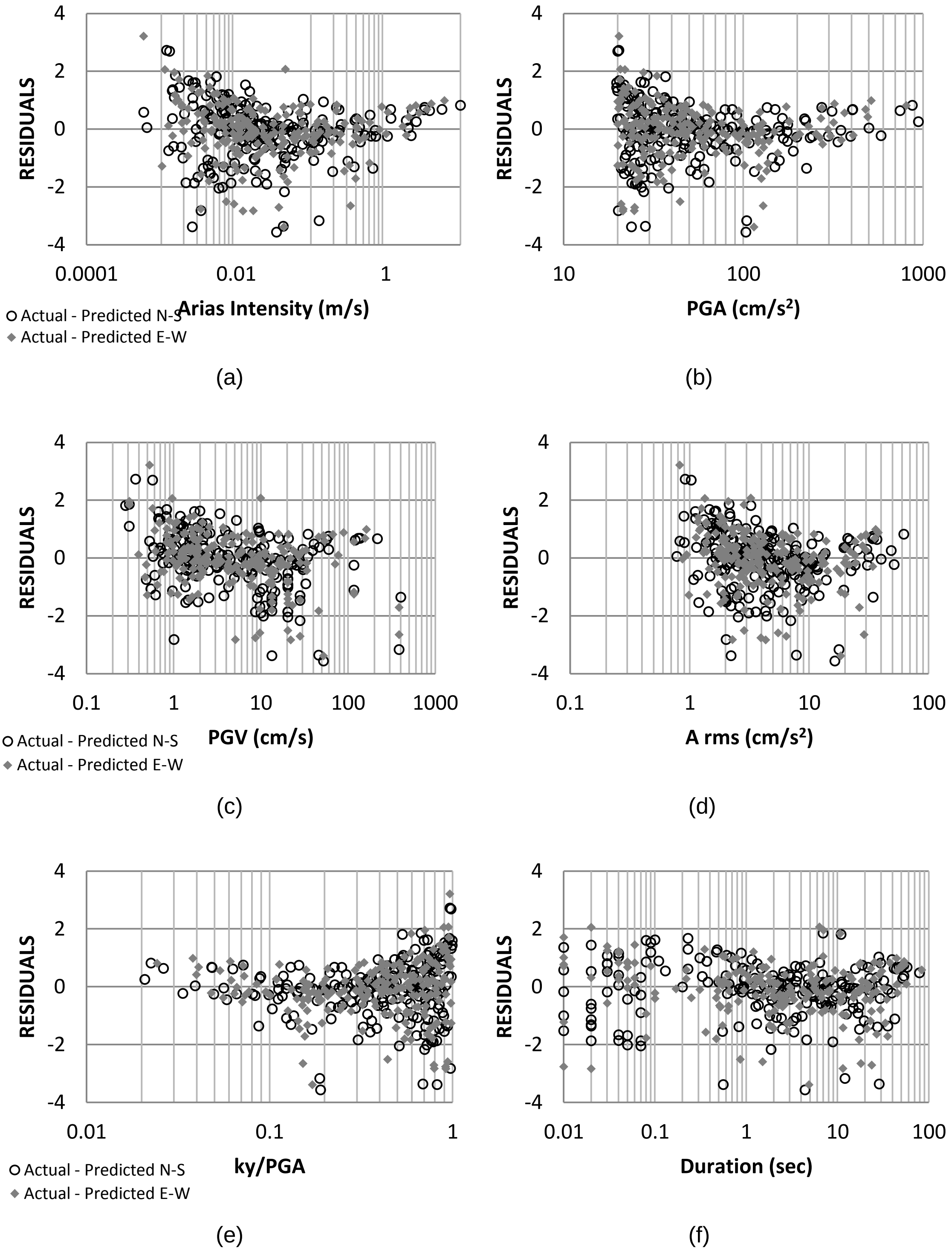

Figure 3.9 Residuals vs a) Arias Intensity, b) PGA, c) PGV, d) A_{rms}, e) k_y/PGA and f) Duration at k_y=0.02g of three parameter vector model (PGA, PGV, I_a) of Saygılı and Rathje (2008)

3.3.5 Bozbey and Gündoğdu (2011)

In this regional model, permanent slope displacements due to seismic loading were investigated using 50 strong motion records from 37 earthquakes occurred in Turkey. Two horizontal components of each recording were analyzed and displacements were calculated for positive and negative polarities; therefore, 4 separate analyses are conducted for every single motion using a C^{++} based computer program called "Quake Analyzer" for a_y/a_{max} values ranging from 0.01 to 0.9 as indicated in Table 3.1.

By using a readily available computer software called "Seismosignal" ground motion intensity measures such as Arias intensity (I_a), root mean square acceleration (A_{rms}), characteristic intensity (I_c), cumulative absolute velocity (CAV) were computed. However, these IMs were not used in this prediction model. Proposed NSB displacement prediction equation is given as:

$$\log(D_n) = -4.39\left(a_y/a_{max}\right) + 1.94 \qquad (R^2 = 0.89) \qquad \mathbf{3.12}$$

where D_n is the NSB displacement in centimeters, a_y is yield acceleration in g, a_{max} is the maximum acceleration in g.

Performance of the NSB displacement predictive model given in Equation 3.12 on the comparison dataset of Turkey is evaluated using the total residual plots for with respect to several ground motion parameters: Arias intensity, PGA, PGV, A_{RMS}, k_y/a_{max} and duration in Figure 3.10(a) to Figure 3.10(f), respectively. As Figures 3.10(a), 3.10(d), and 3.10(f) indicate, model is unable to capture the ground motion properties represented by the Arias Intensity, A_{RMS} or duration and any one of those parameters should be included in the predictive model. Figure 3.10 shows that the model has a misfit form the actual data points even for the only variable included in the model (k_y/a_{max}), therefore, the functional form should be modified. Figures 3.10(b) and 3.10(c) imply that the inclusion of more ground motion parameters (PGA or PGV) would improve the performance of the model.

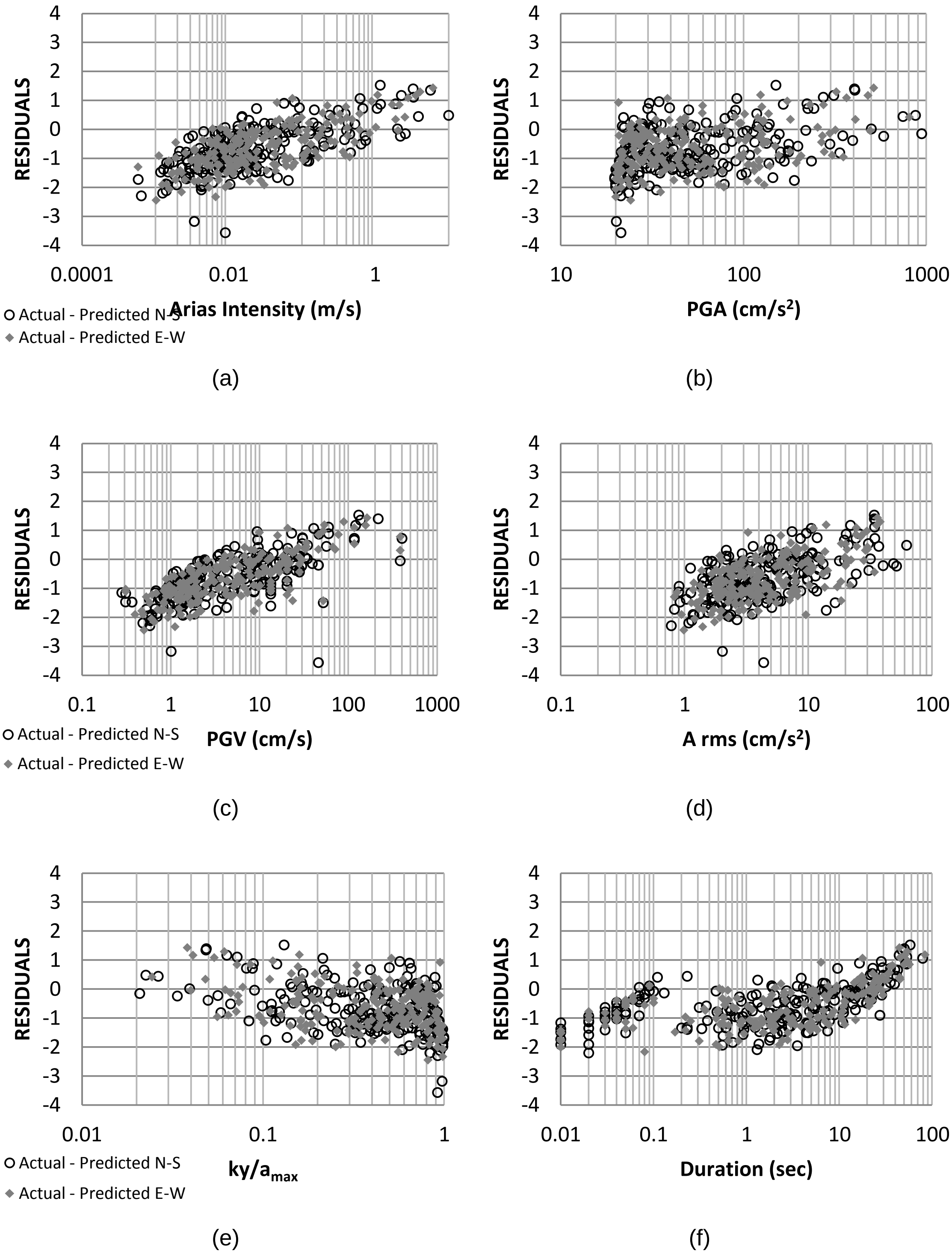

Figure 3.10 Residuals vs. a) Arias Intensity, b) PGA, c) PGV, d) A_{rms}, e) k_y/a_{max} and f) Duration at k_y=0.02g for Bozbey and Gündoğdu (2011)

3.3.6 Hsieh & Lee (2011)

This study employs strong-motion data from the 1999 Chi-Chi earthquake (373 strong-motion records from the mainshock), the 1999 Kocaeli earthquake (41 records), the 1999 Düzce earthquake (20 records), the 1995 Kobe earthquake, the 1994 Northridge earthquake and the 1989 Loma Prieta earthquake. Since the dataset includes strong ground motions from Turkey, model predictions might be compatible with the comparison dataset of Turkey. Hsieh and Lee (2011) had taken Jibson's equations (1993, 1998), which are the basis of Equation 3.6 described above in Jibson (2007), as a starting point for their functional form. Regression analyses have been conducted and the term $\log I_a$ is modified to become $A_c \log I_a$ for the form called "new form I" and an additional $\log I_a$ term is added for the form called "new form II".

8 different predictive equations are presented within two separate forms; containing not only local and global equations for all-soil sites, but also rock sites and soil site equations independently. The global predictive models for the new form I, new form II for all-soils, rock site derived from the new form II and soil site derived from the new form II are shown in Equations 3.13-3.16 respectively:

$$\log(\mathrm{D_n}) = 11.287(\mathrm{a_c})\log(\mathrm{I_a}) - 11.485(\mathrm{a_c}) + 1.948 \pm 0.357 \qquad \mathbf{3.13}$$

$$\log(\mathrm{D_n}) = 0.847\log(\mathrm{I_a}) - 10.62(\mathrm{a_c}) + 6.587\mathrm{a_c}\log(\mathrm{I_a}) + 1.84 \pm 0.295 \qquad \mathbf{3.14}$$

$$\log(\mathrm{D_n}) = 0.788\log(\mathrm{I_a}) - 10.166(\mathrm{a_c}) + 5.95\mathrm{a_c}\log(\mathrm{I_a}) + 1.779 \pm 0.294 \qquad \mathbf{3.15}$$

$$\log(\mathrm{D_n}) = 0.802\log(\mathrm{I_a}) - 10.981(\mathrm{a_c}) + 7.377\mathrm{a_c}\log(\mathrm{I_a}) + 1.914 \pm 0.274 \qquad \mathbf{3.16}$$

where D_n is NSB displacement in centimeters, I_a is Arias intensity in meters per second, and a_c is yield acceleration in g.

Equation 3.13 of the new form I has the least R^2 value (0.84) than the other three equations of the new form II (R^2= 0.89 for Equation 3.14 and 3.15, R^2= 0.91 for Equation 3.16). Therefore, Hsieh and Lee (2011) classified the New form II as much superior to new form I and suggested to be used. For both the site-spesific formulas; soil-site or rock-site, the estimation error is smaller and the goodness of fit is higher. As the landslides are more probable to take place on hillsides, and also the rock site formula is recommended by the researchers to be more practical for the landslide cases, Equation 3.15 is chosen to be the representative prediction equation for this study.

The performance of the NSB displacement predictive model given in Equation 3.15 on the comparison dataset of Turkey is evaluated using the total residual plots for with respect to several ground motion parameters: Arias intensity, PGA, PGV, A_{RMS} and duration in Figure 3.11(a) to Figure 3.11(e), respectively. As Figure 3.11(a) implies that the model has a misfit form the actual data points even for the only variable included in the model (Arias Intensity), therefore, the functional form should be modified. Nonetheless, a clear trend is observed in Figures 3.11(b) through 3.11(e) which indicate that model is unable to capture the ground motion properties represented by the PGA, PGV, A_{RMS} or duration and any one of those parameters should be included in the predictive model. Moreover, Figure 3.11(a) shows that especially for the small Arias Intensity values, the prediction model miscalculates the actual data to a very high extent.

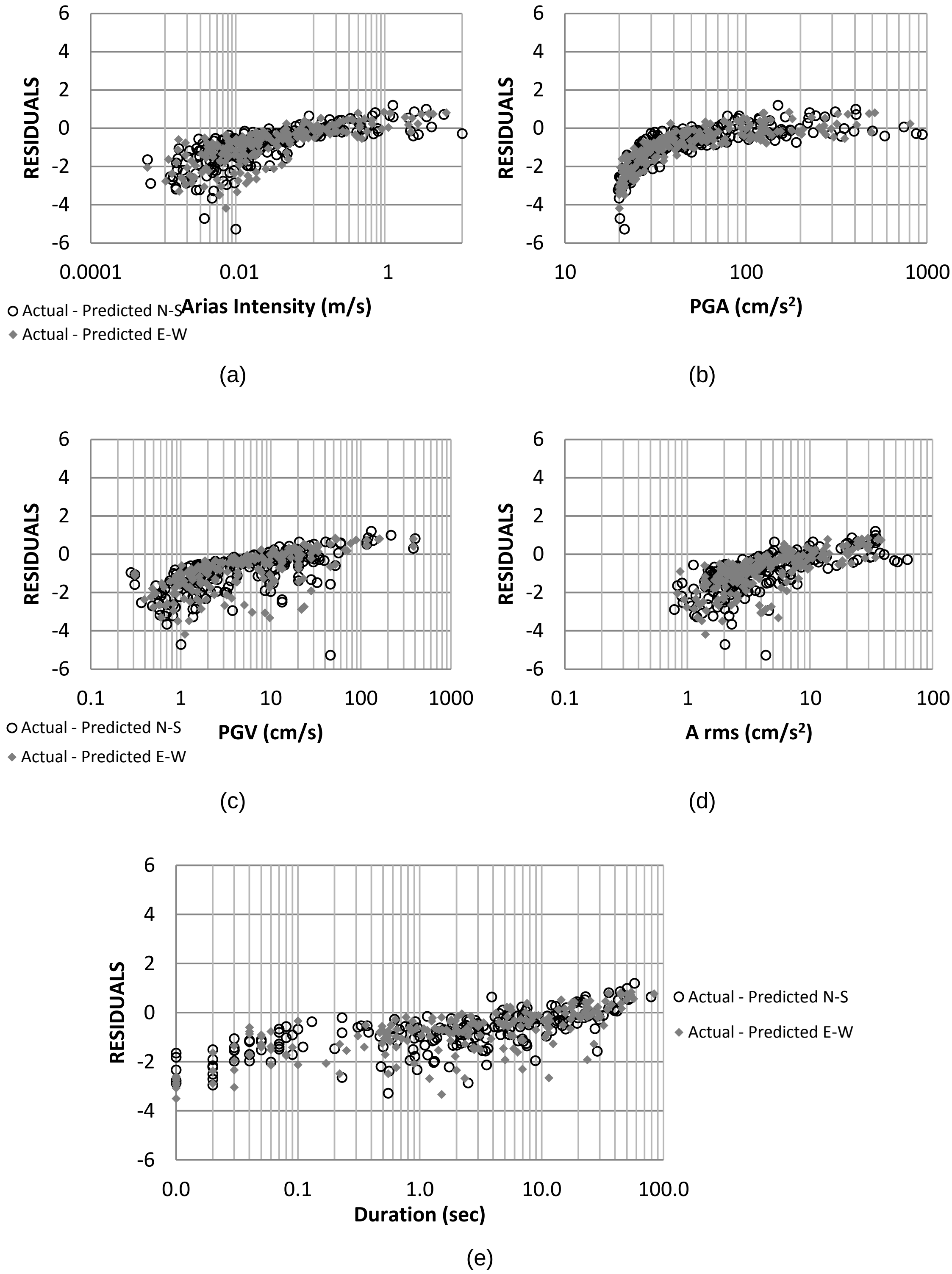

Figure 3.11 Residuals vs. a) Arias Intensity, b) PGA, c) PGV, d) A_{rms} and e) Duration at k_y=0.02g for Hsieh & Lee (2011)

3.3.7 Comparison of the Results

The distributions of the total residuals with respect to the ground motion intensity measures listed in Table 3.2 are presented individually for Watson-Lamprey and Abrahamson (2006) model, Jibson (2007) model, Bray and Travasarou (2007) model, Saygılı and Rathje (2008) two parameter vector model and three parameter vector model, Bozbey and Gündoğdu (2011) model and Hsieh and Lee (2011) model in Figure 3.5 to Figure 3.11, respectively.

Figure 3.12 presents a comparison of all candidate models for a shallow, rigid sliding mass, for a deterministic earthquake scenario of M_w= 7 and R_{rup}= 5 km, and rock site conditions (Vs_{30}= 760 m/s). The values of PGA, PGV and $Sa_{T=1s}$ are determined from Abrahamson and Silva (2008) horizontal GMPE and I_a is determined from Travasarou et al. (2003) prediction model as listed in Table 3.3. Figure 3.12 indicates that Jibson (2007) model predicts the largest displacement values; for the yield acceleration values less than 0.04 g and greater than 0.35g. However for the yield acceleration values between 0.08g and 0.29g, the same model have the smallest displacement predictions. Biggest NSB displacement values are given by Bray and Travasarou (2007) model for all yield accelerations upto 0.33g but the model is not applicable for the yield accelerations above 0.33g for this scenario event since at these large values k_y, median predicted displacement is less than 1 cm and according to their model, displacements less than 1 cm are not of engineering significance. Predictions of Bozbey and Gündoğdu (2011) and Hsieh and Lee (2011) models are very similar for the same yield acceleration values. Both two and three parameter models of Saygılı and Rathje (2008) have average values of NSB displacement, two parameter vector model being greater than three parameter vector model.

Table 3.3 The predicted ground motion parameter for the scenario earthquake of magnitude 7.0 with a distance of 5 km at rock site.

Predictive Model	Calculated Parameters
Abrahamson and Silva (2008)	$\mathrm{PGA} = 0.395\ \mathrm{g}$
	$\mathrm{PGV} = 31.1\ \mathrm{cm/s}$
	$\mathrm{Sa_{T=1s}} = 0.3\ \mathrm{g}$
Travasarou et al. (2003)	$\mathrm{I_a} = 1.07\ \mathrm{m/s}$

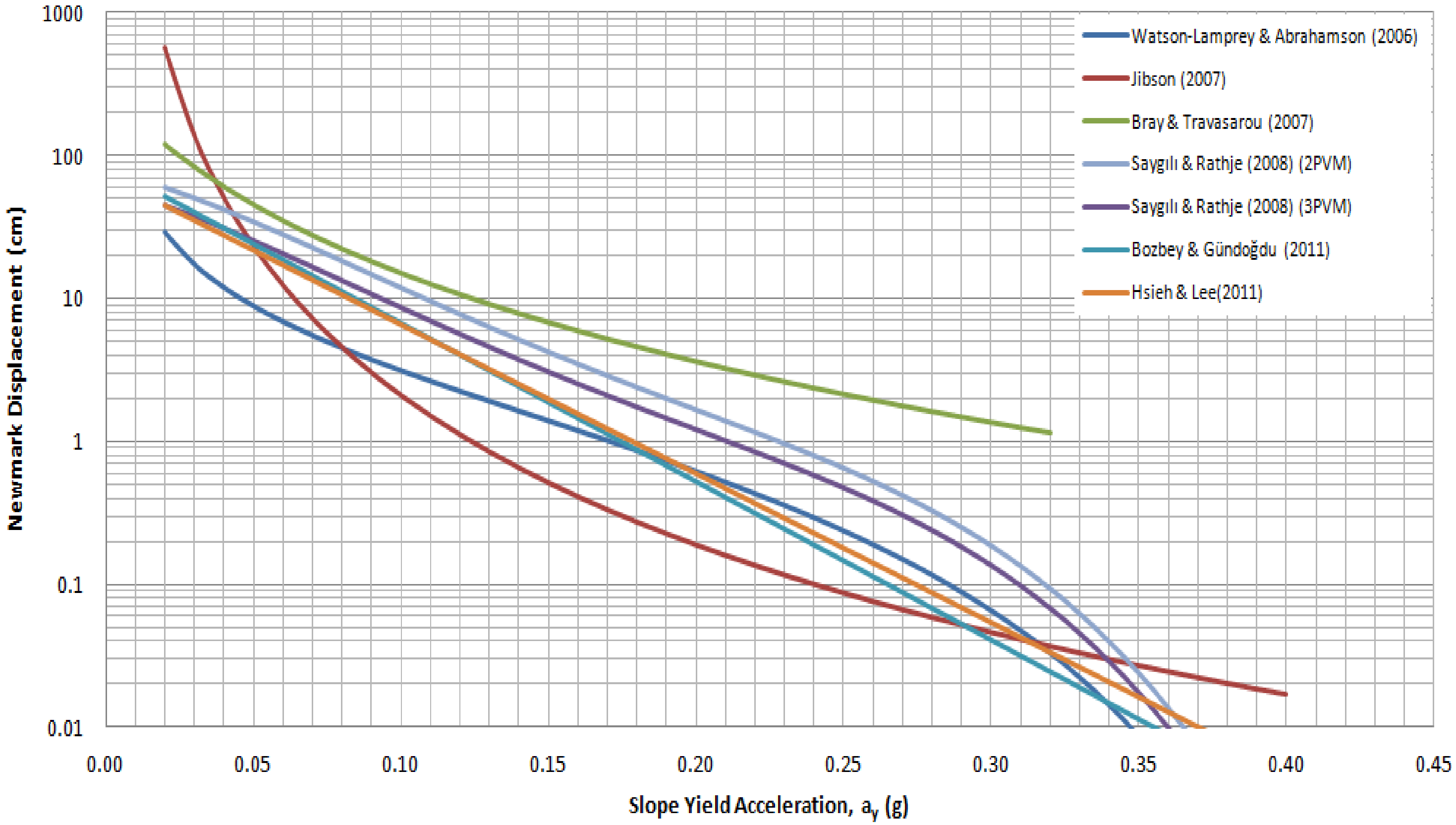

Figure 3.12 Comparison of predictive models for sliding displacement for a deterministic scenario of M_w= 7.0 and R= 5 km at a rock site.

CHAPTER 4

VECTOR-VALUED PROBABILISTIC SEISMIC HAZARD APPLICATION

Because of its geographical location, climatic, geological, and tectonic characteristics, Turkey was always subjected to natural disasters in the past. One of the main hazards encountered during large seismic events is landslides. However, it is very difficult to classify earthquake-induced landslides among other slope instabilities since this classification solely depends on observations and ocular witness. Unfortunately, an inventory for the earthquake-induced landslides is not available in Turkey.

The objective of this chapter is to demonstrate the application of selected NSB displacement prediction model in vector-valued PSHA framework conducted in highly seismic areas around the North Anatolian Fault Zone. Bolu-Düzce Region is selected for the application of the NSB displacement hazard assessment methodology since damaging earthquake-induced landslides were reported in this area during the 1999 earthquakes.

Within the contents of this chapter, the vector hazard concept for NSB displacement prediction model used in this study is described in terms of hazard integral and its main components. The correlation coefficients required to implement the vector-valued PSHA including several ground motion intensity measures used are presented. Fault characterization models and ground motion equations used for this example application is summarized. Finally, the NSB displacement hazard curves for the selected sites are provided for different site conditions and yield accelerations. Moreover, estimated NSB displacement hazard curves are compared to a case history, Bakacak landslide occurred during 1999 Düzce Earthquake.

4.1 VECTOR HAZARD CONCEPT

The basic methodology of PSHA requires computing how often a specified level of ground motion will be exceeded at a site (Cornell, 1968; McGuire, 2004). In other words, in a PSHA, the annual rate of events, also called as the “annual rate of exceedance” that produces a ground motion intensity measure, *IM*, which exceeds a specified level, z, at the site is computed. In traditional PSHA, the equation due to a single seismic source has been given as:

$$\lambda(\mathrm{IM} > \mathrm{z}) = \lambda_{\mathrm{o}} \times \int_{\mathrm{M}} \int_{\mathrm{R}} \mathrm{P}[\mathrm{IM} > \mathrm{z}|\mathrm{M},\mathrm{R}]\, \mathrm{f_M}(\mathrm{M})\, \mathrm{f_R}(\mathrm{M},\mathrm{R}) \times \mathrm{dM} \times \mathrm{dR} \qquad \mathbf{4.1}$$

where $\lambda(\mathrm{IM} > z)$ is the mean annual rate that the ground motion intensity measure (IM) exceeds a given level (z), λ_{o} is the annual rate of earthquakes greater than the minimum magnitude (also called the activity rate), M is magnitude, R is distance, $\mathrm{f_M}(\mathrm{M})$ and $\mathrm{f_R}(\mathrm{M},\mathrm{R})$ are the probability density functions for the magnitude and distance, respectively. $\mathrm{P}[\mathrm{IM} > \mathrm{z}|\mathrm{M},\mathrm{R}]$ represents the probability of observing an *IM* greater than z for the given magnitude and distance.

A PSHA study includes describing a set of earthquake scenarios, predicting the range of ground motions for each of these scenarios, and estimating the rate of each combination of earthquake scenario and ground motion. Each and every scenario is described by the size of the magnitude of the earthquake and the location which defines the distance from the site. The probability that *IM*, to exceed the test value z is obtained from the GMPE. Since the GMPE defines the probabilistic distribution of the ground motion parameters, the scenario must also include a selected value of epsilon, ϵ (Bommer and Abrahamson, 2006), as:

$$\lambda(\mathrm{IM} > z) = \lambda_o \times \int_M \int_R \int_\epsilon \mathrm{P}[\mathrm{IM} > \mathrm{z}|\mathrm{M},\mathrm{R},\varepsilon]\ \mathrm{f_M}\ (\mathrm{M})\ \mathrm{f_R}(\mathrm{M},\mathrm{R})\ \mathrm{f_\varepsilon}(\varepsilon) \times \mathrm{dM} \times \mathrm{dR} \times \mathrm{d}\varepsilon \qquad \mathbf{4.2}$$

where ε is the number of standard deviations above or below the median and $f_\varepsilon(\varepsilon)$ is the probability density function for the epsilon.

To address the ground motion parameters directly, let us remember the NSB displacement predictive equation to be used:

$$ln(D) = (-0.74) + (-4.93)\left(\frac{k_y}{PGA}\right) + (-19.91)\left(\frac{k_y}{PGA}\right)^2 + (43.75)\left(\frac{k_y}{PGA}\right)^3 + (-30.12)\left(\frac{k_y}{PGA}\right)^4 + (-1.30)ln(PGA) + (1.04)ln(PGV) + (0.67)ln(I_a) \pm \epsilon\sigma_{lnD} \qquad \mathbf{4.3}$$

where k_y is the yield acceleration, PGA is the peak ground acceleration in g, PGV is the peak ground velocity in cm/s and I_a is the Arias Intensity in m/s.

For a NSB displacement prediction model that depends on only one *IM*, the hazard integral would be written as:

$$\lambda(\mathrm{D} > z) = \lambda_o \times \int_M \int_R \int_\epsilon \mathrm{P}[\mathrm{D} > \mathrm{z}|\mathrm{D}(\mathrm{IM}(\mathrm{M},\mathrm{R},\varepsilon),\sigma_{\mathrm{lnD}})]\ \mathrm{f_M}\ (\mathrm{M})\ \mathrm{f_R}(\mathrm{M},\mathrm{R})\ \mathrm{f_\varepsilon}(\varepsilon) \times \mathrm{dM} \times \mathrm{dR} \times \mathrm{d}\varepsilon \quad \mathbf{4.4}$$

where $\mathrm{D}(\mathrm{IM}(\mathrm{M},\mathrm{R},\varepsilon))$ is the median NSB displacement for a given intensity measure and σ_{lnD} is the standard deviation for the NSB displacement prediction model.

Since the selected NSB displacement model includes more than one ground motion parameters, a vector hazard integral is required (Bazzurro and Cornell, 2002). For this case, the NSB displacement hazard integral becomes:

$$\lambda(\mathrm{D} > \mathrm{z}) = \lambda_o \int_M \int_R \int_{\epsilon_{PGA}} \int_{\epsilon_{PGV}} \int_{\epsilon_{I_a}} \mathrm{P}\left[\mathrm{D} > \mathrm{z}|\mathrm{D}\left(\mathrm{PGA}(\mathrm{M},\mathrm{R},\varepsilon_{\mathrm{PGA}}),\mathrm{PGV}(\mathrm{M},\mathrm{R},\varepsilon_{\mathrm{PGV}}),\mathrm{I_a}\left(\mathrm{M},\mathrm{R},\varepsilon_{\mathrm{I_a}}\right),\sigma_{\mathrm{lnD}}\right)\right] \times \mathrm{f_M}\ (\mathrm{M})\ \mathrm{f_R}(\mathrm{M},\mathrm{R})\ \mathrm{f}_{\varepsilon_{\mathrm{PGA}}}(\varepsilon_{\mathrm{PGA}})\ \mathrm{f}_{\varepsilon_{\mathrm{PGV}}}(\varepsilon_{\mathrm{PGV}}|\varepsilon_{\mathrm{PGA}})\ \mathrm{f}_{\varepsilon_{\mathrm{I_a}}}\left(\varepsilon_{\mathrm{I_a}}|\varepsilon_{\mathrm{PGV}}\right) \times \mathrm{dM} \times \mathrm{dR} \times \mathrm{d}\varepsilon_{\mathrm{PGA}} \times \mathrm{d}\varepsilon_{\mathrm{PGV}} \times \mathrm{d}\varepsilon_{\mathrm{I_a}} \qquad \mathbf{4.5}$$

where $\varepsilon_{\mathrm{PGA}}$ is the number of standard deviations for PGA, $\varepsilon_{\mathrm{PGV}}$ is the number of standard deviations for PGV, and $\varepsilon_{\mathrm{I_a}}$ is the number of standard deviations for I_a, $\mathrm{f}_{\varepsilon_{\mathrm{PGA}}}(\varepsilon_{\mathrm{PGA}})$ is the probability density function for $\varepsilon_{\mathrm{PGA}}$, $\mathrm{f}_{\varepsilon_{\mathrm{PGV}}}(\varepsilon_{\mathrm{PGV}}|\varepsilon_{\mathrm{PGA}})$ is the probability density function for $\varepsilon_{\mathrm{PGV}}$ conditioned on $\varepsilon_{\mathrm{PGA}}$, and $\mathrm{f}_{\varepsilon_{\mathrm{I_a}}}\left(\varepsilon_{\mathrm{I_a}}|\varepsilon_{\mathrm{PGV}}\right)$ is the probability density function for $\varepsilon_{\mathrm{I_a}}$ conditioned on $\varepsilon_{\mathrm{PGV}}$. The form in Equation 4.5 differs from the formulation given by Bazzurro and Cornell (2002) such that the integral in the equation is over the epsilon values ($\varepsilon_{\mathrm{PGA}}$, $\varepsilon_{\mathrm{PGV}}$ and $\varepsilon_{\mathrm{I_a}}$) rather than ground motion parameters (PGA, PGV, and I_a). While mathematically equivalent, this equation clearly shows that the correlation of the variability of the ground motion values should be considered (Gülerce and Abrahamson, 2010).

The probability density function for the first *IM*, $\mathrm{f}_{\varepsilon_{\mathrm{PGA}}}(\varepsilon_{\mathrm{PGA}})$ is given by the standard normal distribution. However, the probability density function for the second *IM* $\mathrm{f}_{\varepsilon_{\mathrm{PGV}}}(\varepsilon_{\mathrm{PGV}}|\varepsilon_{\mathrm{PGA}})$ is conditioned on the $\varepsilon_{\mathrm{PGA}}$ value and includes the correlation of $\varepsilon_{\mathrm{PGA}}$ and $\varepsilon_{\mathrm{PGV}}$, and so does the probability density function of $\mathrm{f}_{\varepsilon_{\mathrm{I_a}}}\left(\varepsilon_{\mathrm{I_a}}|\varepsilon_{\mathrm{PGV}}\right)$. The $\varepsilon_{\mathrm{PGV}}$ can be defined as a function of $\varepsilon_{\mathrm{PGA}}$ as:

$$\varepsilon_{\mathrm{PGV}} = \rho_{\mathrm{PGV|PGA}} \times \varepsilon_{\mathrm{PGA}} \pm \sigma_{PGV|PGA} \qquad \mathbf{4.6}$$

Similarly, the $\varepsilon_{\mathrm{I_a}}$ can be defined as a function of $\varepsilon_{\mathrm{PGV}}$ as:

$$\varepsilon_{I_a} = \rho_{I_a|PGV} \times \varepsilon_{PGV} \pm \sigma_{I_a|PGV} \qquad \mathbf{4.7}$$

where $\rho_{PGV|PGA}$ is the correlation coefficient between PGA and PGV and $\rho_{I_a|PGV}$ is the correlation coefficient between PGV and Arias Intensity. The covariance of ε_{PGV} with respect to ε_{PGA} and the covariance of ε_{I_a} with respect to ε_{PGV} should be computed from the correlation of normalized residuals for the ground motion prediction model.

To implement the selected prediction model for the NSB displacement in a vector-valued PSHA framework, the correlation coefficients, $\rho_{PGV|PGA}$ and $\rho_{I_a|PGV}$, are required.

The value of the correlation coefficient informs the user about the strength and the nature of the relationship between the ground motion parameters. The correlation coefficient can take any value between −1.0 and +1.0; in which positive values indicate that both *IM*s for a ground motion tend to be large or small (positively correlated), while negative values indicate that when one *IM* is large then the other *IM* parameter tends to be small (negatively correlated). A correlation coefficient of 0 indicates that these two *IM*s are not correlated (Rathje and Saygılı, 2008). The correlation coefficient has a weak dependence on the selected ground-motion prediction model and database (Baker and Cornell, 2006) so values used in the example application will be presented in section 4.2.2 along with the selected GMPEs.

4.2 APPLICATION OF THE PROBABILISTIC NSB DISPLACEMENT HAZARD ANALYSES IN BOLU-DÜZCE REGION

The North Anatolian Fault Zone (NAFZ) is one of the most active fault systems in the world, which lies along Northern Turkey for approximately 1500 kilometers (Barka, 1992). NAFZ system ruptured progressively by large and destructive earthquakes in the last century; in between 1939-1967 (1939 Erzincan, 1943 Tosya-Ladik, 1944 Bolu-Gerede, 1949 Karlıova, 1957 Bolu-Abant, 1967 Mudurnu) had broken almost 900 kilometers of a uniform eastern trace whereas 1999 Kocaeli and Düzce earthquakes ruptured a total fault line of almost 200 kilometers on the west where NAFZ system is divided into branches. A closer look at the density map of settlements subjected to landslides (Figure 4.1) implies that the density of static (not earthquake-induced) landslides increases significantly on the west of the Black Sea Region. Unfortunately, an inventory of earthquake-induced landslides is still not available in Turkey. However, damaging earthquake-induced landslides were reported in the Bolu-Düzce area during the 1999 earthquakes (Aydan and Ulusay, 2002; Süzen and Doyuran, 2004; Bakır and Akış, 2005), coinciding with the landslide prone areas shown in Figure 4.1. Considering these facts, the Bolu-Düzce Region is selected for the application of the NSB displacement hazard assessment methodology.

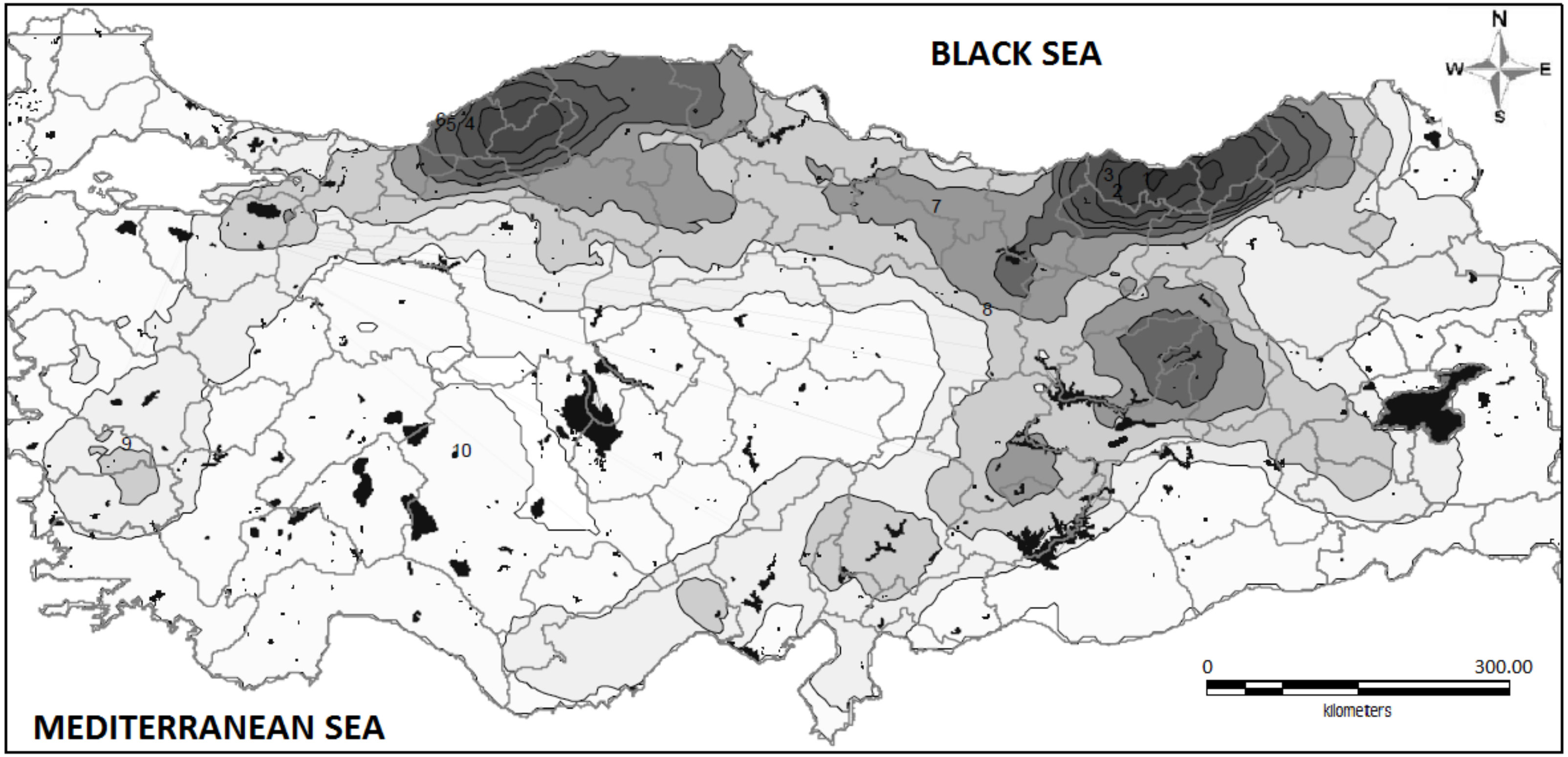

Figure 4.1 Density map of the settlements subjected to landslides in Turkey (The darker the colors, the denser the landslides) (Gökçe et al., 2006).

4.2.1 Seismic Source Characterization

Bolu-Düzce area is a region surrounded by Adapazarı on the west and Gerede on the east including the fault segments of NAFZ ruptured during 1944 Bolu-Gerede, 1957 Abant, 1967 Mudurnu, and 1999 Düzce earthquakes as shown in Figure 4.2. Source characterization models for the seismic sources in the region are implemented from the current PSHA studies conducted for Eastern Marmara by Gülerce and Ocak (2013) and Bolu-Gerede region upto Ilgaz by Levendoğlu (2013), therefore, only a brief summary is provided here for both studies:

- The same approach was adopted with the WG-2003 SF Bay Area Model for seismic source characterization, which is primarily based on characterized faults that are divided into non-overlapping segments. Fault segments in the study area are defined as: Düzce Fault, North Anatolian Fault Zone Southern Strand (NAF S), and 1944 Rupture Zone (Bolu-Gerede Fault) denoted by 1, 2, and 3 in Figure 4.2 respectively.

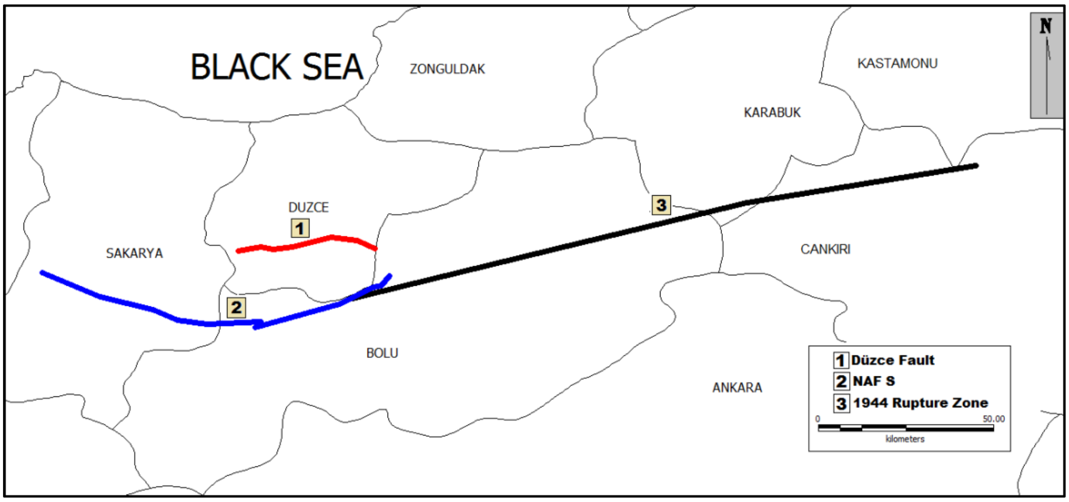

Figure 4.2 Representation of the study area along the main seismic sources.

- Segmentation points and segment lengths are determined by lineament analyses using satellite images of the region (Cambazoğlu et al., 2012) and active fault map of MRE (Emre et al., 2012). Characteristic magnitudes and rupture widths of the fault zone are calculated by the area-magnitude relations recommended by Wells and Coppersmith (1994). Segment geometry, assigned slip rates and characteristic magnitude for each segment that can be seen in Figure 4.3 is tabulated below in Table 4.1.

- Linear fault segments are defined and composite magnitude distribution model (Youngs and Coppersmith, 1985) is used for all seismic sources in the region to properly represent the characteristic behavior of NAFZ without an additional background zone.

- Fault segments, rupture sources and scenarios with fault rupture models are determined and multi segmented rupture scenarios are taken into account. Events in the earthquake catalogue are attributed to the individual seismic sources and scenario weights are determined by moment balancing.

Table 4.1 Segment geometry, assigned slip rates and characteristic magnitude for each segment.

SEGMENTS		RL(km)	RW(km)	SR(mm/yr)	M_{char}
1	Düzce (West)	10.7	35.8	10	6.6
2	Düzce (East)	29.4	35.8	10	7.1
3	Mudurnu	64	12	12	6.9
4	Abant	40	12	15	6.7
5	Abant Lake – Yeniçağa	75	16	20	7.1
6	Yeniçağa – İsmetpaşa	47	16	12	6.9
7	İsmetpaşa – Ilgaz	69	16	20	7.1

RL: Rupture Length, RW: Rupture Width, SR: Slip Rate, M_{char}: Mean Value of the Characteristic Magnitude

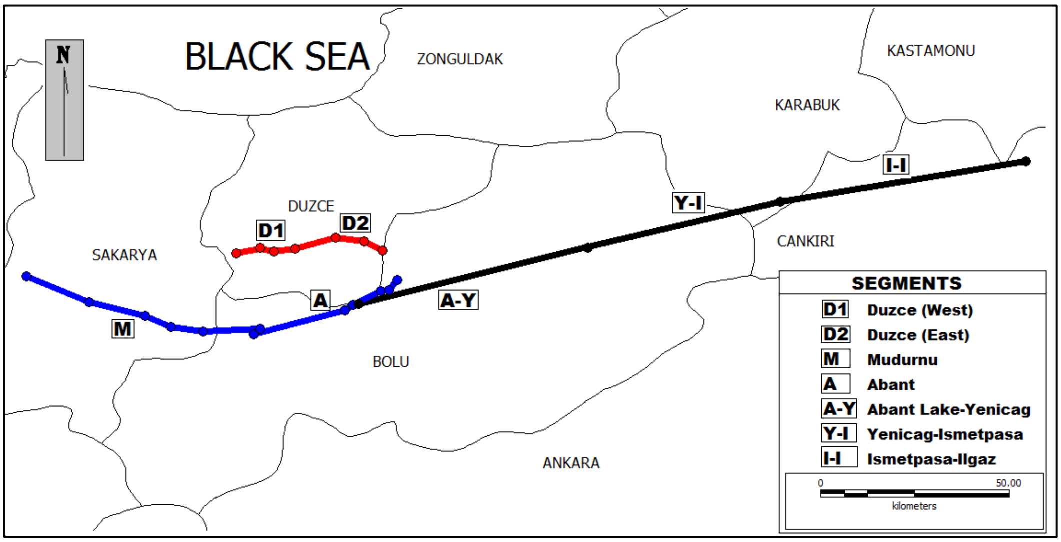

Figure 4.3 Representation of the study area along the segment geometry.

4.2.2 Selection of the Ground Motion Prediction Equations

In PSHA, the Ground Motion Prediction Equations are needed to determine the ground motion parameters for the earthquake scenarios from each and every source considered. The uncertainty presented by the ground motion prediction models is substantially higher than all parameters beside it in the hazard integral; therefore, GMPEs have a prominent influence on the total hazard calculated at the site. Many GMPEs are available in the literature, extending from global ground motion models representing the shallow crustal regions to local ground motion models developed for Turkey.

It has been a controversial topic to choose the ground motion model from one of these groups because both groups have its own advantages and disadvantages. Since local GMPEs are developed from the regional databases, they reflect the regional tectonic characteristics better then the global models. However, as they are based on small datasets with limited ground motion records, the uncertainties in these models are higher than the global models. Contrary to local models, the global models are based on large databases which reduce the epistemic uncertainty in the GMPEs. As the total hazard is evidently affected by the epistemic uncertainty in the ground motion models, therefore the choice shifted to global ground motion models for this study. Considering that the hazard curves obtained using different NGA-W1 models was quite similar in Gülerce and Ocak (2013), only one of the NGA-W1 models, Abrahamson and Silva (2008) model, was used for this example application to decrease the computer run time.

Abrahamson and Silva (2008) model was developed for the rotation-independent average horizontal component from shallow crustal earthquakes based on the updated PEER-W1 strong ground motion database. The PEER-database consists of 3551 recordings from 173 earthquakes that occurred in between 1952 and 2003. The model is applicable to magnitudes 5–8.5, distances 0–200 km, and spectral periods up to 10 seconds including PGA and PGV. The site is parameterized by average shear-wave velocity in the top 30 m (V_{S30}) and the depth to engineering rock (depth to V_S= 1000 m/s) instead of generic site categories (soil and rock). Since the buried ruptures lead to larger short-period ground motions than surface ruptures for the same magnitude and rupture distance, the source term of the model is considered to be dependent on the depth to top-of-rupture in addition to magnitude and style-of-faulting. The standard deviation of the model is magnitude dependent with an inverse ratio as small magnitudes lead to large standard deviation values. The short-period standard deviation model for soil sites is also distance-dependent due to nonlinear site response, with smaller standard deviations at short distances.

The other intensity measure used in the NSB displacement prediction model is Arias intensity. There is no regional model developed for Turkey that predicts the Arias intensity, and also numbers of global Arias intensity prediction models are quite limited. To estimate the Arias intensity, Travasarou et al. (2003) prediction model is selected among the limited number of options for this study. This empirical relationship was developed as a function of magnitude, distance, fault mechanism, and site category based on 1208 recorded ground motion data compiled from 75 earthquakes. The functional form of the model is derived from the point-source model, and the coefficients are determined by using a random-effects model through non-linear regression analyses.

The correlation coefficient between PGA and PGV, $\rho_{\mathrm{PGV|PGA}}$ is calculated using the intra-event residuals of Abrahamson and Silva (2008) model as 0.74 (N. Abrahamson, personal communication, 2012). The correlation coefficient between PGV and Arias intensity, $\rho_{\mathrm{I_a|PGV}}$ could not be calculated since the intra-event residuals of the Travasarou et al. (2003) prediction model is not available. The value given by Rathje and Saygılı (2008) for the Boore and Atkinson (2007) model (0.64) is adopted since the correlation coefficient values are observed to be insensitive to the ground-motion prediction model considered (Baker and Cornell, 2006). To deal with the uncertainty in ground motion predictions, ±3σ value proposed by both models are employed in the PSHA analyses.

4.2.3 NSB Displacement Hazard Curves

Using the fault characterization models and GMPEs defined above, vector-valued probabilistic NSB displacement hazard analyses are performed for selected locations in the area as shown in Figure 4.4. Site 3, Site 6, and Site 7 are arbitrarily chosen sites with the rupture distance of 5 kilometers at the south of the 1944 Earthquake Rupture Zone, since some earthquake-induced landslides were observed below the fault plane (R. Ulusay, personal communication, 2012). Site 6 is located close to the creeping segment (Y-I Segment) of 1944 Earthquake Rupture Zone to check for the effect of slip rate accumulation on the hazard output. Site 4 and Site 5 are parallel to Site 3, but further away from the fault (R_{rup}= 25 km and R_{rup}= 50 km, respectively). Site 1 and Site 2 are located close to the other seismic sources in the area, Site 1 is 5 kilometers away from the NAFZ Southern Strand and Site 2 is 5 kilometers away from the Düzce Fault. The numerical integration of the PSHA integral is conducted with the help of the computer code HAZ40 which was developed by N. Abrahamson for scalar PSHA, modified to perform vector-valued PSHA by Gülerce and Abrahamson (2010), and subjected to further modification to perform three-vector PSHA for this study.

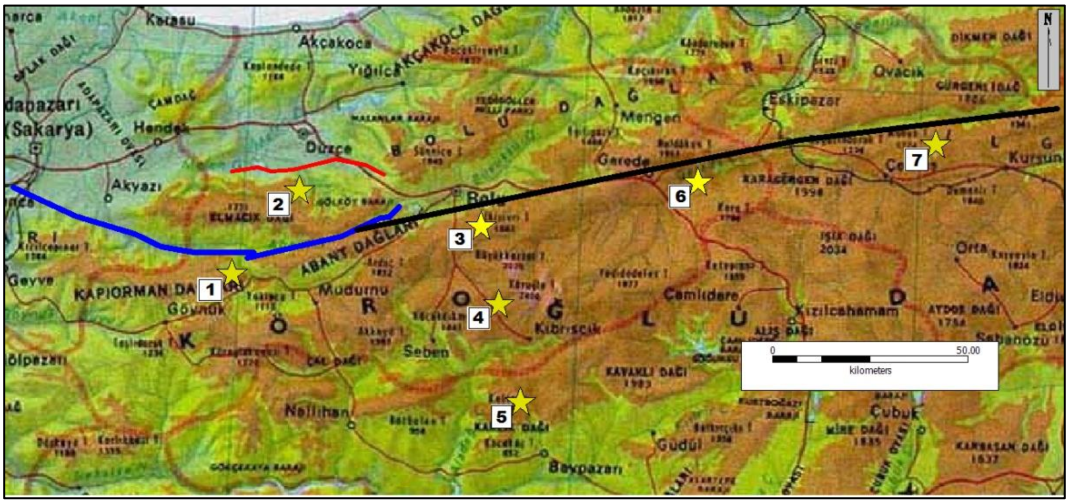

Figure 4.4 The general layout of the sources with the locations where the analyses are preformed.

Figure 4.5 shows the NSB displacement hazard curves for Sites 1, 2,3, 6, and 7 at rock site conditions (V_{s30}= 760 m/s) for the yield acceleration of 0.1g. Since all of these sites are 5 kilometers away from the rupture planes, the hazard curves are very close to each other. The NSB displacement at 10% probability of exceedance in 50 years ($\lambda = 0.0021$) risk level is about 11 cm for Site 1, 9 cm for Site 2, 14 cm for Site 3, 10 cm for Site 6 and 15 cm for Site 7. Similarly, the NSB displacement for 2% probability of exceedance in 50 years ($\lambda = 0.0004$) risk level is 40 cm for Site 1 and Site 6, 32 cm for Site 2, and 48 cm for Sites 3 and 7. The NSB displacement observed at Site 6 is smaller than the others at higher risk levels since that site is close to the creeping segment of the 1944 Rupture Zone and the slip rate of Y-I Segment is smaller than the other seismic sources. NSB displacement hazard at Sites 3 and 7 are larger than the other sites, since these sites are in the near vicinity of the longest segments of the whole system with the highest characteristic magnitudes.

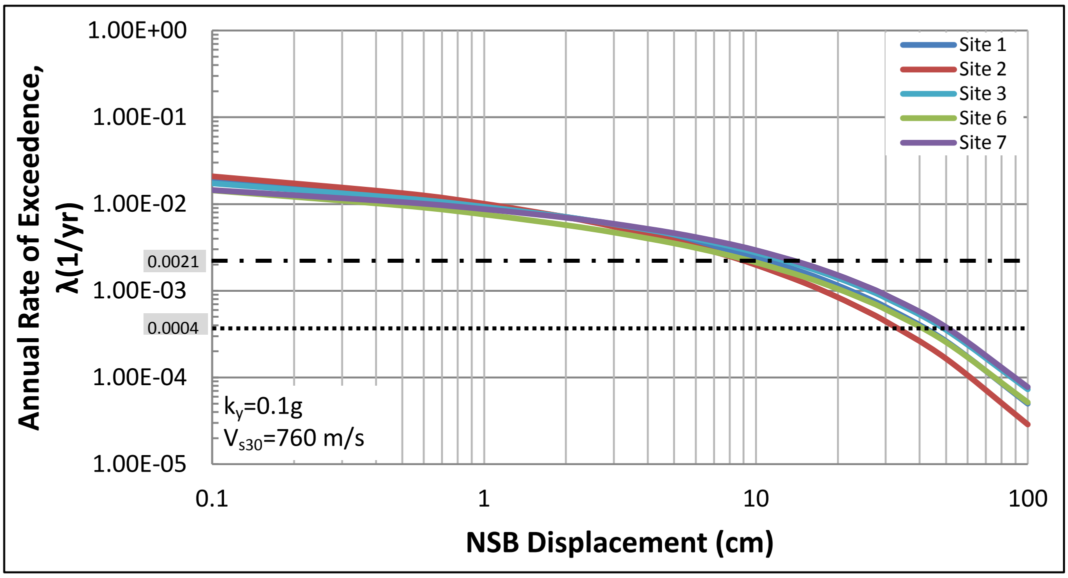

Figure 4.5 NSB displacement hazard curves for Site 1, Site 2, Site 3, Site 6 and Site 7.

The NSB displacement hazard curves for different site conditions at Site 3 for the yield acceleration of 0.1g are presented in Figure 4.6. The shear wave velocity values are chosen according to the NEHRP site class definitions to represent rock site conditions (V_{s30}= 760 m/s), soft rock (or very dense soil) conditions (V_{s30}= 560 m/s), and soil (stiff) site conditions (V_{s30}= 270 m/s). These values are also comparable with the site class definitions of Z1, Z2, and Z3 in the Earthquake Code of Turkey (ECT-2007). The NSB displacement values at 10% probability of exceedance in 50 years ($\lambda = 0.0021$) risk level increases as the V_{s30} value decreases; NSB displacement is about 14 cm for rock, 25 cm for soft rock, and 42 cm for soil site conditions. Similarly the NSB displacement for 2% probability of exceedance in 50 years ($\lambda = 0.0004$) risk level is 48 cm for rock, 88 cm for soft rock, and greater than 100 cm for soil site conditions. According to NSB analogy, slope tends to deform as a single massive block which means a rigid-perfectly plastic stress-strain behavior on a planar failure surface, therefore the rock and soft rock values are more representative for those cases.

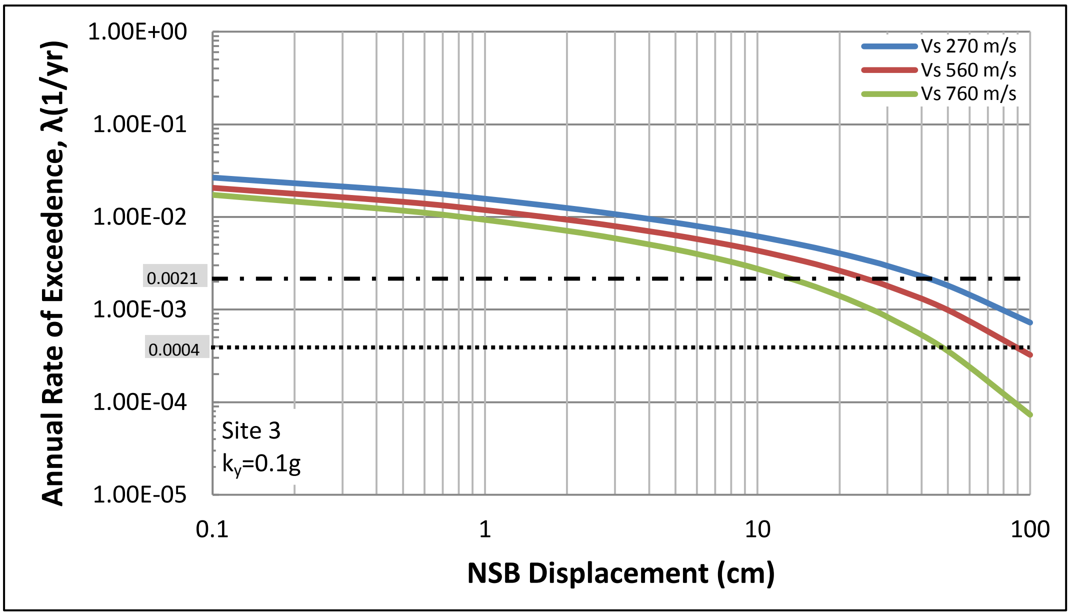

Figure 4.6 NSB displacement hazard curves for different shear wave velocities at Site 3.

The selected yield acceleration and distance to the rupture plane have a considerable effect on the resulting NSB displacement. In Figure 4.7, the NSB displacement hazard curves for Site 3 at rock site conditions, for different yield acceleration values are compared. The NSB displacement for 10% probability of exceedance in 50 years ($\lambda = 0.0021$) is about 2 cm for yield acceleration of 0.2g, but this value increases significantly with decreasing yield acceleration. 14 cm NSB displacement is computed for yield acceleration of 0.1g, and 28 cm is computed for yield acceleration of 0.05g at the same risk level. For a higher risk level 2% probability of exceedance in 50 years ($\lambda = 0.0004$), the NSB displacement values are 18 cm for yield acceleration of 0.2g, 48 cm for yield acceleration of 0.1g, and 75 cm for yield acceleration of 0.05g.

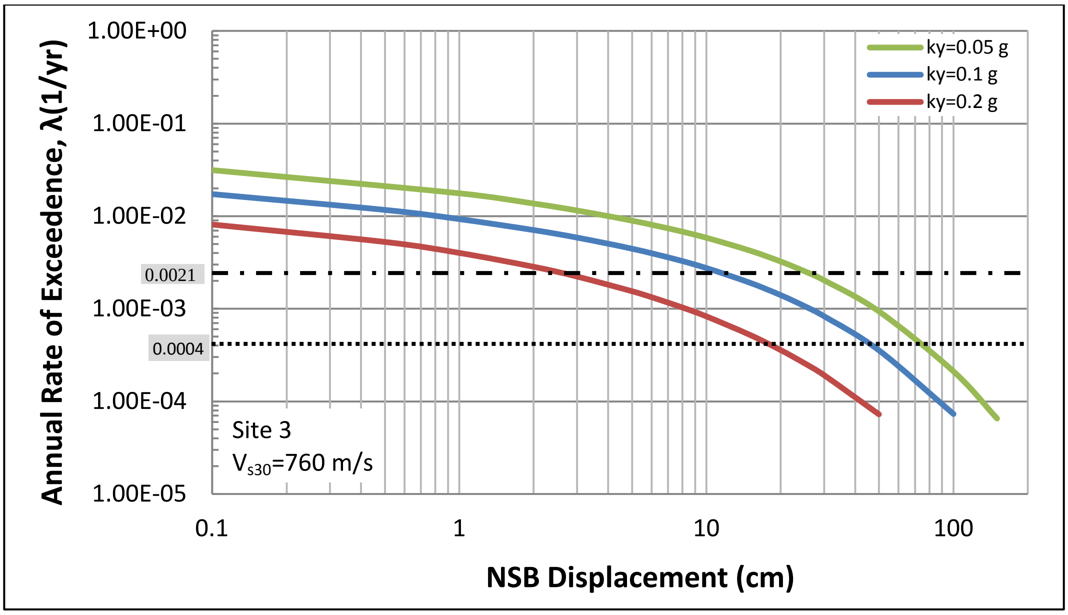

Figure 4.7 NSB displacement hazard curves for different yield acceleration values at Site 3.

NSB displacement hazard curves for Site 3, Site 4 and Site 5, which are located 5, 25 and 50 km away from the nearest source respectively, are presented in Figure 4.8. For rock conditions (V_{s30}= 760 m/s) and with the yield acceleration value of 0.1g, the NSB displacement for 10% probability of exceedance in 50 years ($\lambda = 0.0021$) is 14 cm for Site 3, 1 cm for Site 4, and below 1 cm for Site 5. The NSB displacements for 2% probability of exceedance in 50 years ($\lambda = 0.0004$) is 48 cm for Site 3, 6 cm for Site 4, and about 1 cm for Site 5. These results indicate that earthquake induced landslides hazard is critical for near fault zones, however, the effect diminishes away quickly as the rupture distance increases.

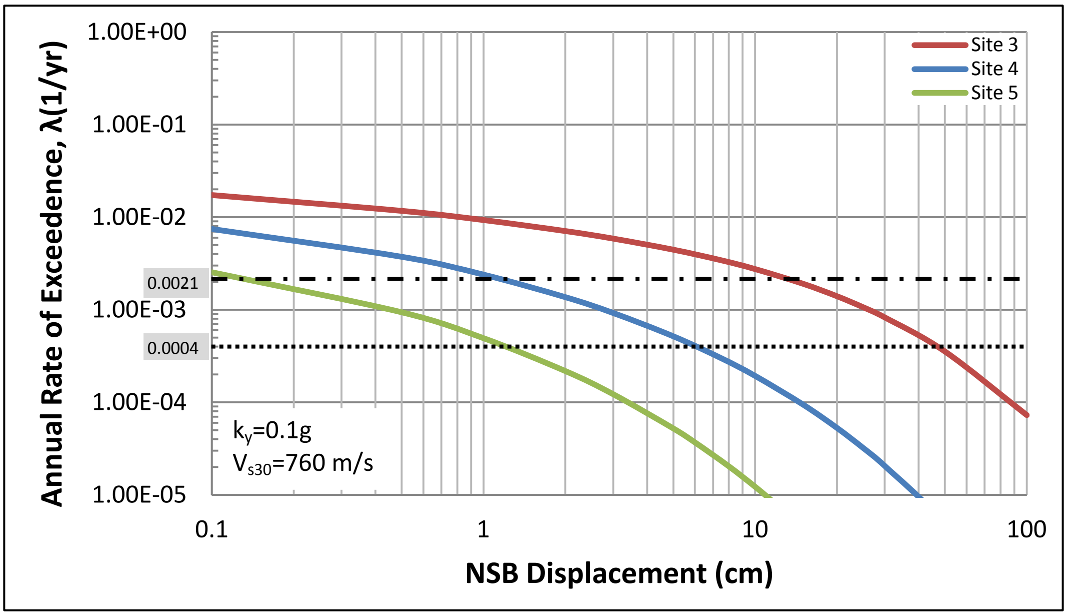

Figure 4.8 NSB displacement hazard curves for Site 3, Site 4 and Site 5.

4.3 COMPARISON OF THE RESULTS WITH AN OBSERVED EVENT: BAKACAK LANDSLIDES DURING 1999 DÜZCE EARTHQUAKE

On 12 November 1999, a devastating earthquake with a moment magnitude of 7.2 had occurred in the Bolu-Düzce Region. In addition to high casualties and damage to different engineering structures, slope and embankment failures on the highway and the country roads had also observed. These failures were particularly occured on the embankments and natural slopes along the southern margin of Düzce Plain, in Bakacak at the northern slopes of Bolu Mountain and on the northern slopes of Asarsuyu Valley (Aydan and Ulusay, 2002). Bakacak landslides extend through Ankara-İstanbul E5 Highway and affected the stability of the highway at several locations (Çetin et. al., 2007).

The slope failures had taken place at the close locations of the fault rupture in highly weathered parts of the granitic and volcanic rock units. A significant part of the failures were classified as shallow-seated circular failures (Aydan and Ulusay, 2002).

Various researchers investigated Bakacak landslides after the earthquake:

- Bakır and Akış (2005) conducted the analyses for the main embankment failure (at Bakacak) that caused the highway to remain out of service. They concluded that the failure of the slope was not in the form of a solid block movement above a localized unique critical surface, but considered a series of slip surfaces that were activated depending on the stresses induced by the inertial forces. Bakır and Akış (2005) also concluded that the Bakacak embankment slope was not particularly suitable for Newmark sliding block type of analyses.

- Aydan and Ulusay (2002) carried out the analyses for the same embankment and the results of the back-analysis based on a pseudo-dynamic approach, showed that the maximum ground acceleration to initiate the failure of the embankment was about 0.125g. Using the N-S components of the strong motion records at the Düzce, Bolu and Mudurnu strong ground motion stations and assuming that the sliding plane is perfectly plastic, dynamic NSB displacement analyses have been performed. The computations with the recording at Mudurnu station, which is located on rock, indicated that the yielding of the embankment was not possible. The maximum acceleration for the N–S direction was about 0.121g, and the static analysis for this value indicated that the slope must be stable. As for computations with the records of Düzce and Bolu stations, which are located on loose alluvial grounds, the NSB displacement values are found to be less than 70 cm for Düzce and 40 cm for Bolu (Aydan and Ulusay, 2002).

- Çetin et al. (2007) also delivered analyses for an existing Bakacak landslide during November 12, 1999 Düzce earthquake. Two cross-sections of the creeping soil slope were numerically modeled and shaken by the recording from Bolu station scaled down to 0.6g, and deconvolved to mudstone bedrock level, as the level of excitation anticipated at the site during the earthquake. The installed inclinometers reveled that the amount of lateral displacements at the chosen cross-sections were 28 cm and 2 cm, respectively. Based on the yield acceleration values, estimated as 0.07 and 0.14g by pseudo static slope stability analyses, Newmark seismic displacements were found to be 26 and 3 cm at the mentioned cross-sections (Çetin et al., 2007).

To compare the vector-valued PSHA results with the case history, 5 more points around the Bakacak landslide (as shown in Figure 4.9) are analyzed using the proposed yield acceleration values at rock site conditions. NSB displacement hazard curves at sites A, B, C, D, and E are presented in Figures 4.10 and 4.11.

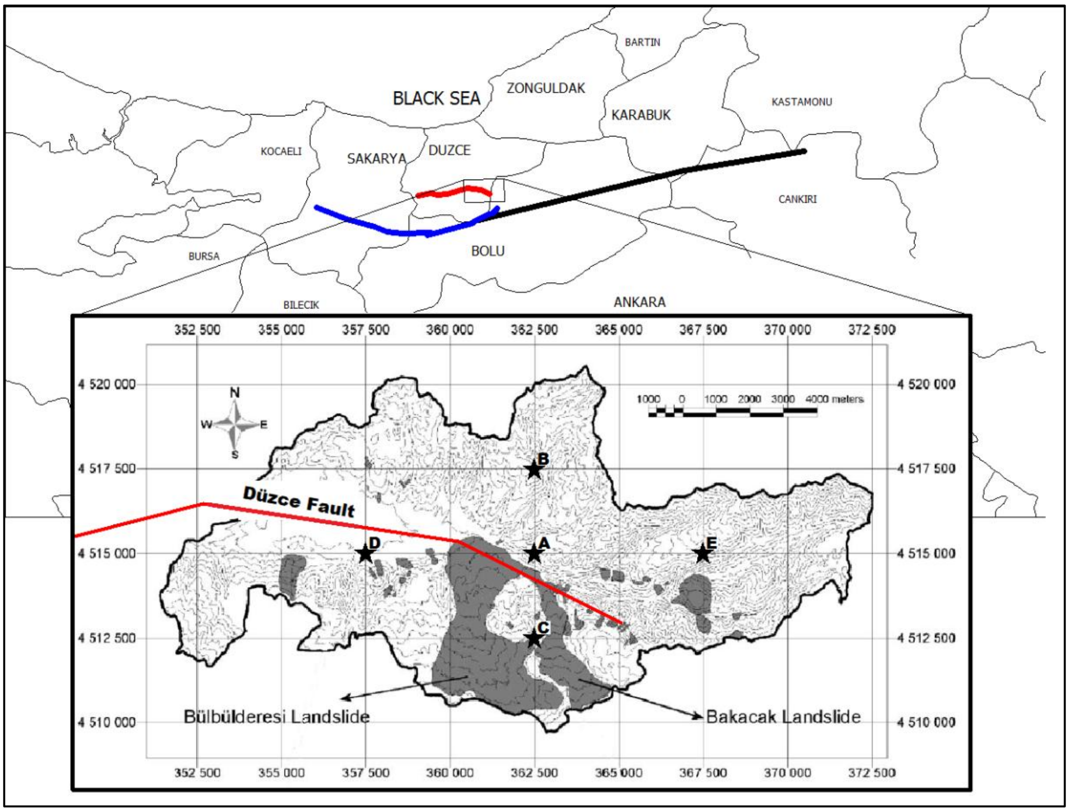

Figure 4.9 The general layout of the study area with the affecting source and the locations where the analyses are preformed (Adopted from Süzen and Doyuran, 2004).

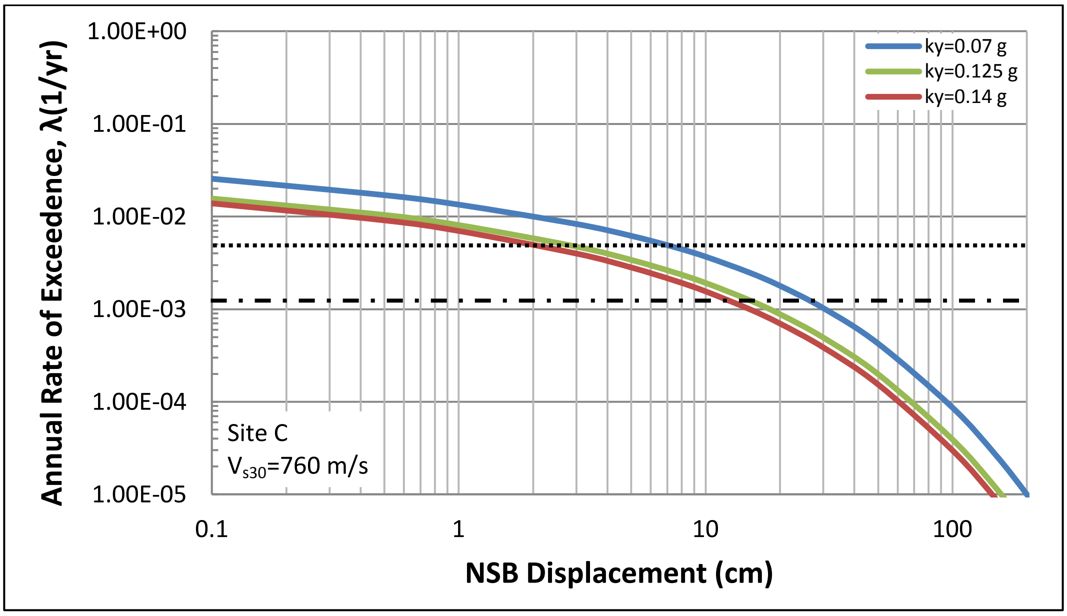

Figure 4.10 NSB displacement hazard curves for the proposed yield acceleration values at Site C.

In Figure 4.10, the NSB displacement hazard curves at Site C, which represent the Bakacak landslide, for different yield acceleration values, which are cited in above mentioned studies, are compared.

Since to use a hazard curve, the risk level in interest has to be employed, there are two unknowns in this comparison: the risk level of the observed event and physical properties of the slope, which is represented by yield acceleration. Therefore, using the inclinometer measurement and the yield acceleration of one cross-section, the risk level is determined, after then the NSB displacements for the other yield accelerations are derived for that specific risk level.

Thus, the risk level at which the NSB displacement is estimated as 2 cm for the yield acceleration of 0.14g, the NSB displacement is found as 7 cm for yield acceleration of 0.07g. On the other hand, the risk level at which the NSB displacement is 28 cm for yield acceleration of 0.07g , the displacement is estimated as 14 cm for yield acceleration of 0.14g The NSB displacements for the same risk levels are 3 cm and 17 cm for yield acceleration of 0.125 g respectively.

The results reveal that; the analyses results are consistent with the inclinometer readings (0.07g and 0.14g), however, for the main embankment failure, the results derived from the analyses seem to be much more smaller than the real case (0.125g), this situation confirms the consideration of Bakır and Akış (2005) as the main embankment slope is not suitable for Newmark type of analysis and also confirms the limitation of the method as the sliding mass behave as a rigid block.

Figure 4.11 shows that, estimated NSB displacements are almost the same for all sites at all risk levels for rock site conditions (V_{s30}= 760 m/s) and for the yield acceleration of 0.125g even if the landslide only occurred at Site C. This result reveals that the method results in the same hazard for all sites at the same distances within the source regardless of the landslide potential. Therefore, these analyses should be combined with landslide susceptibility maps.

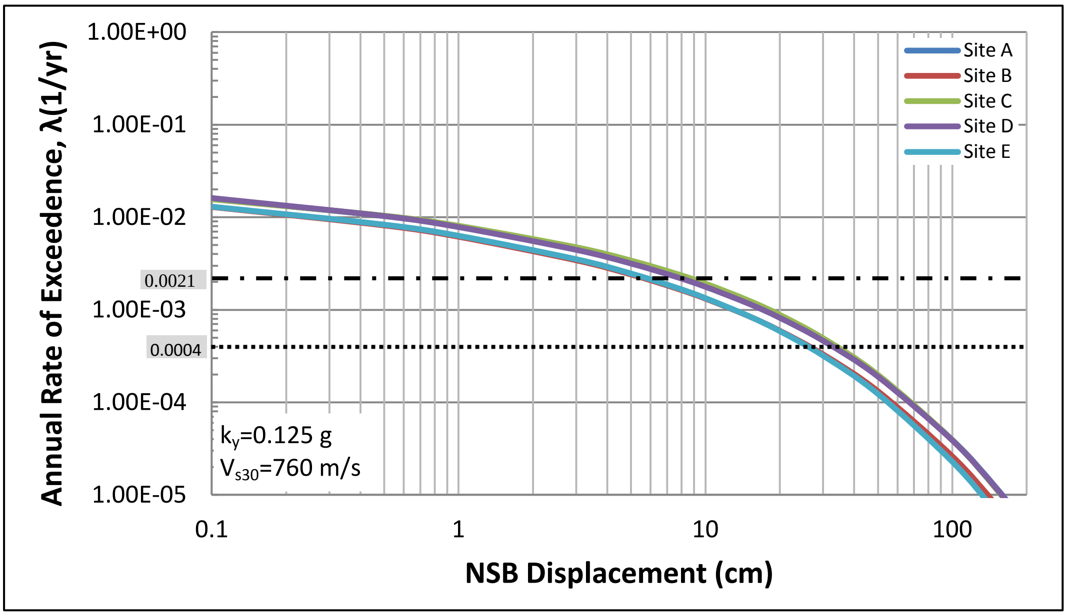

Figure 4.11 NSB displacement hazard curves for Site A, Site B, Site C, Site D and Site E.

CHAPTER 5

SUMMARY AND CONCLUSION

Static stability of slopes (excluding the effects of dynamic forces) can be affected by many factors such as geological and hydrological conditions, topography, climate, weathering, and land use. Having a precise slope stability assessment plays an important role to minimize the damage caused by slope instability and all these factors should be taken into consideration to have an accurate slope stability assessment. In addition to these important factors, disruption of the stability of a slope by an earthquake is also very important which may lead to landslides that can cause loss of life and property. In natural slopes or engineering structures, earthquake motions can generate significant horizontal and vertical dynamic stresses which may increase the shear stresses that may result in exceedance of shear strength on potential failure planes, and slopes become unstable. Consequently, depending on the characteristics of the slopes and ground motion significant damage may be occurred. Since the damage potential of landslides caused by ground shaking is well acknowledged, estimating the earthquake-induced landslide hazards accurately is vital for regional earthquake risk assessment studies.

Seismic evaluations of slope stability show a wide variety from simple pseudostatic procedures to advanced non-linear finite element analyses. For seismically induced permanent displacements, the performance is best evaluated through an assessment of the potential. In practice, two particularly different approaches are available in seismic (or dynamic) evaluation of the slope stability: in *inertia slope stability analysis,* dynamic stresses induced by earthquake shaking are introduced, but in *weakening slope stability analysis,* the effects of dynamic stresses on the strength and stress-strain behavior of slope materials are also taken into account. In other words, inertia slope stability analysis is preferred when material retains its shear strength throughout the ground shaking. However, for the materials that will experience a significant shear strength reduction during an earthquake, weakening slope stability approach is required.

For large-scaled or regional evaluations like this study, the general (inertia) slope stability approach is applicable since the local soil conditions at the analyzed sites are either unknown or roughly estimated and the stress-strain behavior of the soil layers at the sites is not evaluated.

Therefore, in this study, inertia slope stability assessment methods; the pseudostatic approach, Newmark sliding block assessment and Makdisi and Seed (1978) approach are discussed and the main focus was shown on Newmark sliding block method. Newmark's (1965) method models the sliding mass as a rigid friction block that slides on an inclined plane when subjected to base accelerations, representing a strong motion. Landslide displacement is estimated by integrating over the exceeding parts of the threshold acceleration that is required to overcome basal resistance and initiate sliding of an earthquake acceleration-time history twice with respect to time.

The outcome of this analogy is a quantitative measure, the NSB displacement, where larger displacement values indicate higher seismic slope instability risk. NSB displacement is a suitable parameter for risk based approaches, however; NSB analogy requires extensive computational efforts in large-scaled regional applications. The NSB displacement predictive models avoid the obstacle of selecting suitable input time histories and extensive calculations by estimating the NSB displacement using several ground motion intensity measures and links the earthquake scenarios in the PSHA framework to the earthquake induced landslide hazard.

Implementation of global GMPEs, especially the NGA-W1 models developed mainly for California in the other shallow crustal and active tectonic regions is a topic of ongoing discussion. To check the compatibility of the magnitude, distance, and site amplification scaling of NGA-W1 horizontal attenuation relationships with the ground motions that took place in Turkey, Gülerce et al. (2013) modified the lately developed TSMD (Akkar et al., 2010). Analysis results showed that the horizontal NGA-W1 models over predict the ground motions from the earthquakes occurred in Turkey, especially the small magnitude events recorded on stiff soil-rock sites. Therefore, any predictive model based on the global datasets may show a divergence from the regional ground motion characteristics and these global models should be evaluated before being implemented in probabilistic seismic hazard assessment (PSHA) studies in Turkey.

To evaluate the compatibility of these predictive equations to strong ground motion dataset of Turkey first NSB displacements for the local dataset has been computed using a MATLAB routine for both N-S and E-W direction horizontal components of each ground motion and also for each horizontal component, displacements are calculated for both positive and negative polarities (by flipping the time history upside down), and the largest displacement is assigned as the NSB displacement for that horizontal component.

Using model residual analyses, the most appropriate equation is assessed throughout the various equations in the literature: Watson-Lamprey and Abrahamson (2006) model, Jibson (2007) model, Bray and Travasarou (2007) model, Saygılı and Rathje (2008) two parameter vector model and three parameter vector model, Bozbey and Gündoğdu (2011) model and Hsieh and Lee (2011) model. Evaluation of the residual plots indicates that:

- Significant trends are observed in the residual plots of the prediction models that do not include the Arias intensity as an IM, such as Bray and Travasarou (2007) and Bozbey and Gündoğdu (2011). Arias intensity is a measure of earthquake energy given by the integration of squared accelerations over time. Since Arias intensity measures the total acceleration content of the record rather than just the peak value, it provides a more complete characterization of the shaking content of the strong-motion record than does the peak ground acceleration (Jibson, 1993). Arias intensity has also been shown an effective predictor of the earthquake damage potential related to short-period structures, liquefaction (Kayen and Mitchell, 1997), and seismic slope stability (Wilson and Keefer, 1985, Harp and Wilson, 1995). Other related parameters such as duration or root mean square acceleration can be used as a replacement (e.g., Watson-Lamprey and Abrahamson (2006) model) for Arias intensity to improve the prediction performance.

- PGA is an efficient, sufficient and hazard compatible IM and significantly improves the performance of the prediction model. However, the functional form of the PGA term has a substantial effect on the results. Even if the a_y/a_{max} term is generally preferred, additional PGA term decreases the bias in the model predictions as observed in Saygılı and Rathje (2008) model.

- Including more than one IM has a large impact on the model's standard deviation value. In addition to Arias intensity and PGA, a ground motion measure that reflects the small frequency characteristics such as spectral acceleration at T>1 or PGV significantly reduces the variability and standard deviation of the model. Among the models that used a small frequency IM (Watson-Lamprey and Abrahamson (2006), Saygılı and Rathje (2008)), a smaller bias in the residuals is observed in the model that used PGV, indicating that PGV is less effected by the regional ground motion characteristics.

- The models derived based on larger datasets with the help of scaled recordings (Watson-lamprey and Abrahamson (2006), Saygılı and Rathje (2008)) are statistically more stable.

- Jibson (2007), Bray and Travasarou (2007), Bozbey and Gündoğdu (2011), and Hsieh and Lee (2011) models are biased extensively, especially for the small magnitude and small ground shaking levels. More than one of the variables in these prediction models should be revised for applicability in Turkey. Additionally, these models are unable to capture the ground motion properties represented by the Arias intensity, duration, A_{RMS}, PGA or Sa at longer periods and any of those parameters should be included in the predictive model for better performance. Therefore these models are not applicable in the probabilistic NSB displacement hazard assessment studies conducted in Turkey.

- Performance of the Watson-Lamprey and Abrahamson (2006) model is better: no trend in the residual plots is observed except for the spectral acceleration plot. However, there is a constant shift along the zero line; therefore, the constant term of the model should be modified for the Turkish dataset. This result is expected since NGA-W1 models for the horizontal ground motion component significantly overestimated the ground motions in the same comparison dataset (especially for small-to-moderate magnitudes) and those features of the NGA-W1 models should have been adjusted. A similar adjustment may be applied to this method, however, the dataset used in this study is quite small (only 243 ground motions) hence the results may not be very reliable.

- The most compatible model with the regional ground motion characteristics is found as the Saygılı and Rathje (2008) three parameter vector model. It is notable that including more than one IM decreases the variability of the models significantly, however, increases the computer run time substantially.

As a result; 3 parameter-vector model of Saygılı and Rathje (2008) is considered as the most efficient and consistent model for the dataset compiled from strong ground-motion records of Turkey.

A probabilistic seismic hazard framework is used to determine the earthquake-induced landslide hazard for selected sites in Bolu-Düzce Region. To reach that aim, after deciding to use three parameter-vector NSB displacement predictive model of Saygılı and Rathje (2008), the vector hazard approach becomes inevitable.

Therefore, the vector hazard concept for sliding displacement used in this study is summarized in terms of the hazard integral and its main components. The ground motion correlation concept which is required to implement the vector hazard concept with the GMPEs used are presented.

As one of the main components of the probabilistic seismic hazard framework is the seismic source characterization, for the Düzce, Mudurnu-Abant and Abant-Yeniçağa-İsmetpaşa-Ilgaz segments of the North Anatolian Fault Zone (NAFZ) are considered to be the study area since some real cases had been observed for the area. The activity rates, magnitude distribution functions, and reccurrence models of the seismic source models, which were incorporated in hazard calculations, are based on the available studies of Gülerce and Ocak (2013) and Levendoğlu (2013).

Using the GMPEs of Abrahamson and Silva (2008) and Travasarou et al. (2003) with the NSB displacement prediction equation, which is determined to be appropriate for local conditions, for different located sites, for different soil conditions, and for different yield acceleration values, NSB displacement Hazard Curves for the selected region are provided. Moreover, due to well known landslide occurrences, a case study was conducted around Bakacak region. Many researchers have examined the area and gathered some valuable results. In this study, these results are used to verify the results obtained from the analyses.

Examining the hazard curves, following results have been assessed:

- The sites, located near Yeniçağ-İsmetpaşa segment of the 1944 rupture, are less prone to hazard in sites located near the Abant Lake-Yeniçağ and İsmetpaşa-Ilgaz segments since it is the creeping segment of the 1944 rupture zone and the slip rate of Yeniçağ-İsmetpaşa segment is smaller than the other seismic sources.

- Keeping in mind that NSB displacement analogy is more appropriate for rocks, as the shear wave velocity of the soil decreases, estimated sliding displacement increases. Soft rocks classified as Class C according to NEHRP or Z2 according to TEC are subjected to larger displacement hazards than rocks classified as Class B according to NEHRP or Z1 according to TEC due to the site amplification models embedded in GMPEs.

- Sliding displacements are observed in close vicinities of fault planes upto 5 km, but far field regions does not pose a serious threat for seismically induced displacements.

- When an engineering slope is planned to be designed using a risk-based approach with the allowable displacement limits for the design, physical properties of the slope should be investigated, the yield acceleration should be estimated properly and the probabilistic NSB displacement hazard assessment curve for the real yield acceleration value should be used.

It is obligatory to underline that these results presented here are only valid for soils that can behave as a rigid block and obeying the perfectly plastic behavior and other slope instability mechanisms was not considered.

No ground intensity measure; Arias intensity, PGA, PGV, etc. can represent the complete characteristics of the acceleration time history. This uncertainty is included in the standard deviations of the NSB displacement predictive models.

It is worth to remember that the only parameter used in the analyses that reflect the site effects is yield acceleration, other than the yield acceleration no other geological-geomorphological factors that can be correlated with the slope instability are considered in this study.

As a future recommendation, landslide hazard maps can be developed by choosing landslide sensitive sites that are going to be analyzed with the help of aerial photographs. Since as such, the method works independently to “susceptibility” concept giving the same hazard level for the same distances with the source.

REFERENCES

Abrahamson, N. A., Silva, W., 2008. Summary of the Abrahamson & Silva NGA ground-motion relations, Earthquake Spectra, Volume 24, No. 1, 67-97.

Akkar, S., Çağnan, Z., Yenier, E., Erdoğan, E., Sandıkkaya, M.A., Gülkan, P., 2010. The recently compiled Turkish strong-motion database: preliminary investigation for seismological parameters, Journal of Seismology, 14, 457-479.

Ambraseys, N.N., Menu, J.M., 1988. Earthquake-induced ground displacements, Earthquake Engineering and Structural Dynamics 16, 985-1006.

Ambraseys, N.N. Srbulov, M. 1994. Attenuation of Earthquake-Induced Displacements, *Earthquake Engineering and Structural Dynamics*, V. 23, 467-487.

Ambraseys, N.N., Srbulov, M., 1995. Earthquake induced displacements of slope, Soil Dynamics and Earthquake Engineering 14, 59-71.

Arias, A., 1970. A measure of earthquake intensity. Hansen, R.J. (Ed.), Seismic Design for Nuclear Power Plants. Massachusetts Institute of Technology Press, Cambridge, MA, 438-483.

Aydan, Ö., Ulusay, R., 2002. Back-analysis of a seismically induced highway embankment failure during the 1999 Düzce earthquake, Environmental Geology 42, 621-631.

Baker, J. W., Cornell, C. A., 2006. Correlation of response spectral values for multicomponent ground motions, Bulletin of the Seismological Society of America, Vol. 96, No. 1, 215-227.

Bakır, B.S., Akış¸ E., 2005. Analysis of a highway embankment failure associated with the 1999 Düzce, Turkey earthquake, Soil Dynamics and Earthquake Engineering 25, 251-260.

Barka, A. A., 1992. The North Anatolian Fault Zone, Annales Tectonicae, Volume VI, 164-195.

Bazzurro, P., Cornell, C. A., 2002. Vector-valued probabilistic seismic hazard analysis (VPSHA), in Proceedings. 7th U.S. National Conference on Earthquake Engineering, paper #61, Boston, Massachusetts.

Bommer, J. J., Abrahamson N. A., 2006. Why do modern seismic hazard analyses often lead to increased hazard estiamtes?, Bulletin of Seismological Society of America 96 (6), 1967-1977.

Boore, D. N., Atkinson, G., 2007. Boore-Atkinson NGA ground motion relations for the geometric mean horizontal component of peak and spectral ground motion parameters, PEER Rep. 2007/01, Pacific Earthquake Engineering Research Center, University of California, Berkeley.

Bozbey, İ., Gündoğdu, O., 2011. A methodology to select seismic coefficients based on upper bound ''Newmark'' displacements using earthquake records from Turkey, Soil Dynamics and Earthquake Engineering, 31, 440-451.

Bray, J. D., 2007. Chapter 14: Simplified seismic slope displacement procedures, Proc., Earthquake Geotechnical Engineering, 4th Int. Conf. on Earthquake Geotechnical Engineering-Invited Lectures, K. D. Pitilakis, ed., Vol. 6, Springer, New York, 327-353.

Bray, J. D., Rathje, E. M., 1998. Earthquake-induced displacements of solid-waste landfills, Journal of Geotechnical and Geoenvironmental Engineering 124 (3), 242-253.

Bray, J.D., Travasarou, T., 2007. Simplified procedure for estimating earthquake-induced deviatoric slope displacements, Journal of Geotechnical and Geoenvironmental Engineering 133 (4), 381-392.

Bray, J.D., Travasarou, T., 2009. Pseudostatic coefficient for use in simplified seismic slope stability evaluation, Journal of Geotechnical and Geoenvironmental Engineering 135 (9), 1336-1340.

California Division of Mines and Geology, 1997. Guidelines for evaluating and mitigating seismic hazards in California, California Division of Mines and Geology Special Publication vol. 117, 74 pp.

Cambazoğlu, S., Akgün, H., Koçkar, M. K., 2012. Preparation of a Line Source Model for Probabilistic Seismic Hazard Analyses of Düzce Province, Turkey, 15th World Conference on Earthquake Engineering, Portugal, Lisbon.

Chopra, A. K., 1966. Earthquake effects on dams, Ph.D. dissertation, University of California, Berkeley.

Cornell, C. A., 1968. Engineering seismic risk analysis, Bulletin of Seismological Society of America 58, 1583-1606.

Cornell, C. A., Luco, N., 2001. Ground motion intensity measures for structural performance assessment at near-fault sites, Proc., U.S.– Japan Joint Workshop and Third Grantees Meeting, U.S.–Japan Cooperative Research on Urban EQ. Disaster Mitigation, Seattle.

Crespellani, T., Madiai, C., Vannucchi, G., 1998. Earthquake destructiveness potential factor and slope stability, Geotechnique 48 (3), 411-419.

Çetin, K. Ö., Horoz, A., Erol, O., Unutmaz, B., 2007. Seismic performance of existing Bakacak landslide after 1999 Düzce (Turkey) Earthquake, XIV. European Conference on Soil Mechanics and Geotechnical Engineering, Madrid, Spain.

Day, R. W., 2002. Geotechnical Earthquake Engineering Handbook, McGraw Hill Handbooks.

Del Gaudio, V., Pierri, P., Wasowski, J., 2003. An approach to time-probabilistic evaluation of seismically induced landslide hazard, Bulletin of the Seismological Society of America 93, 557–569.

Emre, Ö., Duman, T. Y., Özalp, S., 2012. Active Fault Map of Turkey, MRE, Ankara.

Franklin, A. G., Chang, F. K., 1977. Permanent displacements of earth embankments by Newmark sliding block analyses, Miscellaneous Paper Vol. S-71-17, U.S. Army Corps of Engineers Waterways Experiment Station, Vicksburg, Mississippi.

Gökçe, O., Demir, A., Özden, Ş., 2006, Distribution of Landslide Residential Units in Turkey and Investigation in GIS Environment (in Turkish), Proceedings, 1st Landslide Symposium, CGETB, Trabzon, 24-40.

Gülerce, Z., Abrahamson, N.A., 2010. Vector-valued Probabilistic Seismic Hazard Assessment for the Effects of Vertical Ground Motions on the Seismic Response of Highway Bridges, Earthquake Spectra Vol. 26 (4), 999-1016.

Gülerce, Z., Kargıoğlu, B., Abrahamson, N. A., 2013. Turkey-Adjusted NGA-W1 Ground Motion Prediction Models, Earthquake Spectra (submitted).

Gülerce, Z., Ocak, S., 2013. Probabilistic Seismic Hazard Assessment of Eastern Marmara Region, Bulletin of Earthquake Engineering (submitted).

Gündoğdu, Ö., 2008. Determination of lateral displacement in slopes using Newmark analysis (in Turkish), Master Thesis, Civil Eng. Program, İstanbul University, Institute of Science, İstanbul, Turkey.

Harp, E. L., Wilson, R. C., 1995. Shaking intensity for rock falls and slides: evidence from 1987 Whittier Narrows and Superstition Hills earthquake strong-motion records, Bulletin of the Seismological Society of America 85 (6), 1739-1757.

Hsieh S., Lee C., 2011. Empirical estimation of the Newmark displacement from the Arias intensity and critical acceleration, Engineering Geology 122, 34-42.

Hynes-Griffin, M. E., Franklin, A. G., 1984. Rationalizing the seismic coefficient method, US Army Corps of Engineers Waterways Experiment Station, GL-84-13, Miscellaneous Paper, 37.

Jibson, R. W., 1993. Predicting earthquake-induced landslide displacements using Newmark's sliding block analysis, Transportation Research Record 1411, 9-17.

Jibson, R. W., Keefer, D. K., 1993. Analysis of the seismic origin of landslides: examples from the New Madrid seismic zone, Geological Society of America Bulletin 105, 521–536.

Jibson, R. W., Harp, E. L., Michael, J. M., 1998. A method for producing digital probabilistic seismic landslide hazard maps: an example from the Los Angeles, California area. US Geological Survey Open-File Report 98-113.

Jibson, R. W., Harp, E. L., Michael, J. M., 2000. A method for producing digital probabilistic seismic landslide hazard maps, Engineering Geology 58, 271-289.

Jibson, R. W., 2007. Regression models for estimating coseismic landslide displacement, Engineering Geological 91, 209-218.

Kayen, R. E, Mitchell, J. K., 1997. Assessment of liquefaction potential during earthquakes by Arias intensity, Journal of Geotechnical and Geoenvironmental Engineering 123 (12), 1162-1174.

Keefer, D. K., 1984. Landslides caused by earthquakes, Geological Society of America Bulletin, 95 (4), 406-421.

Keefer, D. K., 2001. Landslides, in learning from earthquakes-preliminary observations on the southern Peru earthquake of June 23, 2001. Earthquake Engineering Research Institute Special Report, 4-5.

Kramer, S. L., 1996. Geotechnical Earthquake Engineering, Prentice Hall.

Krinitzsky, E. L., Gould, J. P., Edinger, P. H., 1993. Fundamentals of Earthquake-Resistant Construction, John Wiley and Sons, New York.

Kumar, K., 2008. Basic Geotechnical Earthquake Engineering, New Age International (P) Limited, Publishers.

Levendoğlu, M., 2013. Probabilistic Seismic Hazard Assessment of İsmet Paşa – Abant Segments of North Anatolian Fault Using Improved Seismic Source Models, Master Thesis, Civil Eng. Program, Middle East Technical University, Ankara, Turkey, expected to be completed in January 2013.

Lin J. S., Whitman R. V., 1986. Earthquake-induced displacements of Sliding Blocks, Journal of Geotechnical Engineering, Vol. 112, No.1, 44-59.

Luzi, L., Pergalani, F., 1999. Slope instability in static and dynamic conditions for urban planning: the “Oltre Po Pavese” case history (Regione Lombardia-Italy), Natural Hazards 20, 57-82.

Makdisi, F. I., Seed, H. B., 1978. Simplified Procedure for Estimating Dam and Embankment Earthquake - Induced Deformations, Journal of the Geotechnical Engineering Division, ASCE, Vol. 104 (GT7), 849-867.

Mankelow, J.M., Murphy, W., 1998. Using GIS in the probabilistic assessment of earthquake triggered landslide hazards, Journal of Earthquake Engineering 2, 593-623.

Marcuson, W. F., 1981. Moderator’s report for session on “Earth dams and stability of slopes under dynamic loads.”, International Conference on Recent Advances in Geotechnical Earthquake Engineering and Soil Dynamics, Vol. 3, 1175.

McGuire, R. K., 2004. Analysis of seismic hazard and risk, EERI Monograph, Earthquake Engineering Research Center, Oakland, California.

Miles, S.B., Ho, C.L., 1999. Rigorous landslide hazard zonation using Newmark's method and stochastic ground motion simulation, Soil Dynamics and Earthquake Engineering 18, 305-323.

Miles, S.B., Keefer, D.K., 2000. Evaluation of seismic slope performance models using a regional case study, Environmental & Engineering Geoscience 6, 25-39.

Miles, S.B., Keefer, D.K., 2001. Seismic Landslide Hazard for the City of Berkeley, California, US Geological Survey Miscellaneous Field Studies Map MF-2378.

Newmark, N. M., 1965. Effects of earthquakes on dams and embankments.Geotechnique, 15 (2), 139-160.

Rathje, E. M., Saygılı, G., 2006. A vector hazard approach for Newmark sliding block analysis, Proceedings, New Zealand Workshop on Geotechnical Earthquake Engineering Workshop, 20–23 November, University of Canterbury, Christchurch, New Zealand, 205-216.

Rathje, E. M., Saygılı, G., 2008. Probabilistic seismic hazard analysis for the sliding displacement of slopes: Scalar and vector approaches, Journal of Geotechnical and Geoenvironmental Engineering 134 (6), 804-814.

Rodríguez-Marek, A., Bray, J. D., and Abrahamson, N. A., 2001. An Empirical Geotechnical Seismic Site Response Procedure, Earthquake Spectra 17(1), 65-87.

Sarma, S. K., 1975. Seismic stability of earth dams and embankments. Geotechnique Vol. 25, 743-761.

Saygılı, G., Rathje, E. M., 2008. Empirical predictive models for earthquake-induced sliding displacements of slopes, Journal of Geotechnical and Geoenvironmental Engineering 134 (6), 790-803.

Stewart, J. P., Liu, A. H., Choi, Y., 2003. Amplification factors for Spectral Acceleration in Tectonically active Regions, Bulletin of the Seismological Society of America Vol. 93 (1), 332-352.

Süzen, M. L., Doyuran, V., 2004. Data driven bivariate landslide susceptibility assessment using geographical information systems: a method and application to Asarsuyu catchment, Turkey, Engineering Geology 71, 303-321.

Taniguchi, E., Sasaki, Y., 1986. Back analysis of landslide due to Naganoken Seibu Earthquake of September 14, 1984, Proceedings, XI ISSMFE Conference, Session 7B, San Francisco, California, University of Missouri, Rolla.

Terzaghi, K., 1950. Mechanisms of landslides, Engineering Geology (Berkey) Volume, Geological Society of America.

Travasarou, T., Bray, J.D., Abrahamson, N.A., 2003. Empirical attenuation relationship for Arias intensity, Earthquake Engineering and Structural Dynamics 32, 1133-1155.

Ulusay, R., Tuncay, E., Sönmez, H., Gökçeoğlu, C., 2004. An attenuation relationship based on Turkish strong motion data and iso-acceleration map of Turkey, Engineering Geology 74, 265-291.

Varnes, D. J., 1978. Slope movement types and processes, in Schuster, R. L., and Krizek, R. J., eds., Landslides-Analysis and control: National Academy of Sciences Transportation Research Board Special Report 176, 12-33.

Watson-Lamprey, J., Abrahamson, N. A., 2006. Selection of ground motion time series and limits on scaling, Soil Dynamics and Earthquake Engineering, 26 (5), 477-482.

Wells, D. L., K. J. Coppersmith, 1994. New empirical relationships among magnitude, rupture length, rupture width, rupture area, and surface displacement, Bulletin of the Seismological Society of America 84 (4), 974-1002.

Wieczorek, G.F., Wilson, R.C., Harp, E.L., 1985. Map showing slope stability during earthquakes in San Mateo County California: US Geological Survey Miscellaneous Investigations Map I-1257-E, scale 1:62,500.

Wilson, R.C., Keefer, D.K., 1983. Dynamic analysis of a slope failure from the 6 August 1979 Coyote Lake, California Earthquake, Bulletin of the Seismological Society of America 73, 863-877.

Wilson, R.C., Keefer, D.K., 1985. Predicting areal limits on earthquake-induced landsliding, In Evaluating Earthquake Hazards in the Los Angeles Region, J. I. Ziony, ed. Professional Paper 1360. U.S. Geological Survey, Reston, VA, 317-345.

Yegian, M.K., Marciano, E.A., Ghahraman, V.G., 1991. Earthquake induced permanent deformations: probabilistic approach, Journal of Geotechnical Engineering 117, 35-50.

Youngs, R. R., K. J. Coppersmith, 1985. Implications of fault slip rates and earthquake recurrence models to probabilistic seismic hazard estimates, Bulletin of the Seismological Society of America 75 (4), 939-964.